

REPORT DOCUMENTATION PAGE				Form Approved OMB NO. 0704-0188	
<p>The public reporting burden for this collection of information is estimated to average 1 hour per response, including the time for reviewing instructions, searching existing data sources, gathering and maintaining the data needed, and completing and reviewing the collection of information. Send comments regarding this burden estimate or any other aspect of this collection of information, including suggestions for reducing this burden, to Washington Headquarters Services, Directorate for Information Operations and Reports, 1215 Jefferson Davis Highway, Suite 1204, Arlington VA, 22202-4302. Respondents should be aware that notwithstanding any other provision of law, no person shall be subject to any penalty for failing to comply with a collection of information if it does not display a currently valid OMB control number.</p> <p>PLEASE DO NOT RETURN YOUR FORM TO THE ABOVE ADDRESS.</p>					
1. REPORT DATE (DD-MM-YYYY) 24-11-2009		2. REPORT TYPE Technical Report		3. DATES COVERED (From - To) 24-Nov-2009 -	
4. TITLE AND SUBTITLE Electromagnetic resonances of a wire on an earth-air interface				5a. CONTRACT NUMBER W911NF-07-1-0509	
				5b. GRANT NUMBER	
				5c. PROGRAM ELEMENT NUMBER 0464A7	
6. AUTHORS John M. Myers, Sheldon S. Sandler, and Tai Tsun Wu				5d. PROJECT NUMBER	
				5e. TASK NUMBER	
				5f. WORK UNIT NUMBER	
7. PERFORMING ORGANIZATION NAMES AND ADDRESSES Harvard College Office of Sponsored Research 1350 Massachusetts Ave. Holyoke 727 Cambridge, MA 02138 -				8. PERFORMING ORGANIZATION REPORT NUMBER	
9. SPONSORING/MONITORING AGENCY NAME(S) AND ADDRESS(ES) U.S. Army Research Office P.O. Box 12211 Research Triangle Park, NC 27709-2211				10. SPONSOR/MONITOR'S ACRONYM(S) ARO	
				11. SPONSOR/MONITOR'S REPORT NUMBER(S) 52943-EL.1	
12. DISTRIBUTION AVAILABILITY STATEMENT Approved for public release; federal purpose rights					
13. SUPPLEMENTARY NOTES The views, opinions and/or findings contained in this report are those of the author(s) and should not be construed as an official Department of the Army position, policy or decision, unless so designated by other documentation.					
14. ABSTRACT A promising approach to detecting roadside bombs attached to command wires is the electromagnetic sensing and identification of the wires. The lowest five resonant frequencies of the wires, along with the widths of the resonances, can serve as a "fingerprint" for finding the wires. A first major step toward exploiting this fingerprint is to calculate the resonances and their widths for a straight wire on a flat interface between a homogeneous earth and air. The calculation of resonances requires extending the theory of the linear antenna to deal with a wire on the					
15. SUBJECT TERMS Command wires on the earth; theory of linear antenna on planar interface; integral equations of Pocklington and Hallen type; resonant frequencies; numerical calculations; Galerkin method; MATLAB computer programs.					
16. SECURITY CLASSIFICATION OF:			17. LIMITATION OF ABSTRACT UU	15. NUMBER OF PAGES	19a. NAME OF RESPONSIBLE PERSON Tai Wu
a. REPORT UU	b. ABSTRACT UU	c. THIS PAGE UU			19b. TELEPHONE NUMBER 617-495-7844

Report Title

Electromagnetic resonances of a wire on an earth-air interface

ABSTRACT

A promising approach to detecting roadside bombs attached to command wires is the electromagnetic sensing and identification of the wires. The lowest five resonant frequencies of the wires, along with the widths of the resonances, can serve as a "fingerprint" for finding the wires. A first major step toward exploiting this fingerprint is to calculate the resonances and their widths for a straight wire on a flat interface between a homogeneous earth and air. The calculation of resonances requires extending the theory of the linear antenna to deal with a wire on the interface between two dielectric media, which we accomplish here. Complex-valued resonant frequencies are defined as those for which a certain homogeneous integral equation for the current in the wire on the interface has non-zero solutions. By applying a Galerkin procedure we obtain approximate numerical solutions for the resonant frequencies and their widths. A table of resonances is given for the case of a relative dielectric constant equal to 4 and for three values of the ratio of the wire radius to wire length. MATLAB computer programs for determining resonant frequencies and widths for other parameter values are included.

School of Engineering and Applied Sciences
Harvard University Cambridge, Massachusetts 02138



Electromagnetic Resonances of a Wire on an Earth-Air Interface

by

John M. Myers, Sheldon S. Sandler, and Tai Tsun Wu (PI)

TECHNICAL REPORT

FOR

ARMY RESEARCH OFFICE GRANT W911NF-07-1-0509

November 12, 2009

US Army Research, Development and Engineering Command
Army Research Office
P.O. Box 12211
Research Triangle Park, NC 27709-2211

Electromagnetic Resonances of a Wire on an Earth-Air Interface

John M. Myers, Sheldon S. Sandler, and Tai Tsun Wu (PI)
School of Engineering and Applied Sciences,
Harvard University, Cambridge, Massachusetts 02138

TECHNICAL REPORT

FOR ARMY RESEARCH OFFICE GRANT W911NF-07-1-0509

NOVEMBER 12, 2009

Abstract—A promising approach to detecting roadside bombs attached to command wires is the electromagnetic sensing and identification of the wires. The lowest five resonant frequencies of the wires, along with the widths of the resonances, can serve as a “fingerprint” for finding the wires. A first large step toward exploiting this fingerprint is to calculate the resonances and their widths for a straight wire on a flat interface between a homogeneous earth and air. The calculation of resonances requires extending the theory of the linear antenna to deal with a wire on the interface between two dielectric media, which we accomplish here. Complex-valued resonant frequencies are defined as those for which a certain homogeneous integral equation for the current in the strip on the interface has non-trivial solutions. By applying a Galerkin procedure we obtain approximate numerical solutions for the resonant frequencies and their widths. A table of resonances is given for the case of a relative dielectric constant ϵ_r of the earth equal to 4 and for three values of the ratio of wire radius a to wire length h . MATLAB computer programs for determining resonant frequencies and widths for other parameter values are included.

TABLE OF CONTENTS

Table of Contents	i
Lists of Illustrations and Tables	iii
Section I. Introduction and Summary of Results.....	1
Section II. Formulation.....	5
Section III. Zeros in the Fourier Transform of E_x	8
Section IV. Integral Equation for the Current	14
Section V. Method of Determining Resonances	17
1. Galerkin subspace for resonances with symmetric and antisymmetric currents	19
2. Resonances	20
3. Scaling to $h = 1$	22
Section VI. Numerical Analysis of Resonances.....	22
1. Summary of the kernel transformed for numerical calculation.....	24
2. Putting the kernel in a form suitable for numerical analysis	26
Acknowledgment.....	27
Appendix A. Comparison with Homogeneous Medium.....	27
Appendix B. Form of Series Expansion for $F_1(\xi, y)$	28
Appendix C. Case of k_1 Close to k_2	29

Appendix D. Integrations for I_{cn} and I_{sn}	30
Appendix E. Evaluation of \mathbf{K}_1 , \mathbf{K}_2 , and \mathbf{K}_3	32
1. Evaluation of $\mathbf{K}_2(x)$	33
2. Evaluation of \mathbf{K}_3	36
3. Evaluation of the integral in \mathbf{K}_{31}	37
4. Evaluation of $\mathbf{K}_{32}(x)$	40
5. Study of a simplified integral relevant to \mathbf{G}_j and to $\mathbf{K}_2(0)$	42
6. Integral for $\mathbf{K}_2(0)$	43
7. Pole for residue contribution to \mathbf{G}_j	43
8. Evaluating zeros in Fourier transform of electric-field kernel	44
Appendix F. MATLAB Programs	45
References	63

LISTS OF ILLUSTRATIONS AND TABLES

Figure 1. Resonant scattering from wire; $\epsilon_r = 4$, $a/h = 10^{-4}$	4
Figure 2. Resonant scattering from wire; $\epsilon_r = 4$, $a/h = 10^{-5}$	5
Figure 3. Resonant scattering from wire; $\epsilon_r = 4$, $a/h = 10^{-6}$	6
Figure 4. Schematic diagram of the antenna geometry.	7
Figure 5. A usual choice of the first sheet in the ξ -plane. With this and a number of similar choices, the zeros of $\tilde{E}(\xi, y)$ at $\xi = k_0$ and $\xi = -k_0$ are on the first sheet.	15
Figure 6. Two cases of the kernel when $k_1/k_2 = 2$ and $k_2h = 5$; $a/h = 10^{-4}$ and $a/h = 10^{-6}$	17
Figure 7. Kernel $\mathbf{K}(x)$ compared with Hallén kernel $H(x)$ for case of $k_2h = 5$, $k_1/k_2 = 2$, and $a/h = 10^{-4}$	18
Figure 8. Integration region on (x', y) -plane.	32
Figure 9. Integration paths Γ_{j1} and Γ_{j2} on complex κ -plane.	41
Table 1. Complex values of k_2h at resonance n	4
Table 2. Sample values of the k_0^2/k_2^2 as a function of k_2a and k_1/k_2	14

I. INTRODUCTION AND SUMMARY OF RESULTS

The need to detect and identify command wires that control roadside bombs raises the problem of determining an electromagnetic signature of command wires that run along the surface of the earth. We study such a wire (or wire pair) in terms of the theory of linear antennas. The theory of linear antennas in a single homogeneous medium was well developed over fifty years ago in terms of integral equations [1]; however, the problem of characterizing command wires calls for extending this theory to deal with two media at a planar interface, and the extra medium raises a whole new set of problems, requiring a substantial development of technique.

In terms of the Maxwell equations that define electromagnetism, here we report on the needed technique and its application to the determination of resonant frequencies of a straight thin wire (or wire pair) on a flat interface between earth and air or, more generally, between two homogeneous lossless media, each characterized by a given dielectric constant. In case of a thin wire in a homogeneous medium, the shape of the cross section is unimportant. For example, with perfect conductors, a wire consisting of a flat strip of width $4a$ and negligible thickness is electromagnetically essentially the same as a circular wire of radius a . This insensitivity to cross-sectional shape holds also for a thin wire or wire pair on the boundary between two different dielectric media. Therefore one is free to pick a shape of the cross section, and the analytically convenient shape is a flat, perfectly conducting strip of length $2h$, width $4a$, and zero thickness. We assume the strip is located in a plane interface, thought of as horizontal, between a medium below (earth) with a dielectric constant k_1 and a medium above (air) with a dielectric constant k_2 . The problem is to find the first five resonant frequencies for electromagnetic radiation scattered by this thin strip as functions of the parameters a , h , k_1 , and k_2 ; the width of each resonance is also to be determined. For a single homogeneous medium, our understanding both of the linear antenna and the related scattering problem comes mostly from the Hallén integral equation. From this integral equation, in which the vector potential plays a central role, it follows that the current on such an antenna is approximately sinusoidal, especially when the

antenna is thin. Furthermore, the wave number for this approximately sinusoidal current is that of the surrounding medium. In contrast, for the present case of a linear antenna on an interface, there is no useful definition of a vector potential, which complicates formulating the problem. When the wire involves two media with distinct propagation constants, the questions arise:

1. Is the current along the wire approximately sinusoidal; and
2. if so, what is its wave number?

Based on the known expression for the electric field emanating from a point current element located on and parallel with the interface [2], integral equations of both the Pocklington type and the Hallén type can be formulated, but with a more complex kernel that introduces qualitatively new features, associated physically with the complexity of paths by which energy can propagate near an interface. As described below, it turns out that the current near resonance is approximately sinusoidal, but, even when both media are lossless, with a complex-valued propagation constant.

Even for a single medium the Hallén and the Pocklington equations for antenna problems are notoriously difficult to solve either analytically or numerically, and indeed have been solved accurately only for a few special cases, such as the center-driven antenna [1]. Recently, however, we defined resonances in terms of special frequencies in the complex plane at which the homogeneous Pocklington equation has non-zero solutions. We then determine the first few resonances approximately by use of a Galerkin method, without the necessity of solving any integral equation. We checked that the application of this method to the case of a wire in a single homogeneous medium showed agreement with known resonances given in Ref. [1] (in which the current distribution along the wire is symmetric).

We proceed as follows:

1. In Sec. II, taking the strip to run along the x -axis, we start with the expression of the electric field $E_x(x, y)$ along the strip generated by a current element on the strip, obtained as the inversion of a Fourier transform. This expression lays the groundwork

for a kernel in an integral equation, once one finds a way to avoid a non-integrable singularity.

2. In Sec. III we find the complex-valued zeros in the Fourier transform of $E_x(x, y)$ with respect to x , denoted $\tilde{E}_x(\zeta, y)$. These zeros play a role similar to the zeros in the Fourier transform for the homogeneous case, and in the same way they allow one to obtain an integral equation of the Pocklington type for the current in the strip, arranged to evade non-integrable singularities.
3. In Sec. IV we derive a suitably symmetrized integral equation of the Pocklington type for the current in a thin strip on the interface. Important implications are: (1) that the current along the wire near resonance is indeed sinusoidal, and (2) we have the propagation constant of this approximately sinusoidal current.
4. In Sec. V we define the complex-valued resonant frequencies as the frequencies at which the homogeneous integral equation for the current in the strip has non-zero solutions. Approximate equations for the resonant frequencies, suitable for numerical calculation, are obtained by use of a Galerkin procedure.
5. In Sec. VI, the equations are rearranged to facilitate numerical computation, largely by changing integration contours to avoid undue oscillation in the integrands of various integrals.
6. Appendix F gives the MATLAB programs that generate numbers from the rearranged equations to provide numerical values for the first five resonant frequencies, along with the width of each resonance (which is simply related to the imaginary part of the complex-valued resonant frequency).

As an example of resonant frequencies, here are the results from the analysis given below (computed with the MATLAB programs in Appendix F) for the case of earth having a dielectric constant 4 times that of free space, leading to $k_1/k_2 = 2$. The first five complex-valued resonant frequencies for three cases of a/h , the ratio of wire thickness to wire length,

are given in Table 1. The propagation constant in air is $k_2 = 2\pi f/c$ where f is the frequency in Hertz and $c \approx 3 \times 10^8$ m/s is the speed of light. (Note that an even resonance number n corresponds to anti-resonance for the impedance of a center-driven antenna.)

Figures 1, 2, and 3 show the resonances implied by Table 1 as a function of frequency.

TABLE 1: Complex values of $k_2 h$ at resonance n

n	$a/h = 10^{-4}$	$a/h = 10^{-5}$	$a/h = 10^{-6}$
1	0.956824- i 0.047401	0.965436- i 0.038153	0.970820- i 0.031885
2	1.934017- i 0.079959	1.947398- i 0.063718	1.955503- i 0.052866
3	2.905922- i 0.115751	2.925628- i 0.091953	2.937355- i 0.076062
4	3.872673- i 0.153152	3.900158- i 0.121734	3.916394- i 0.100618
5	4.837435- i 0.190228	4.873157- i 0.151508	4.894259- i 0.125246

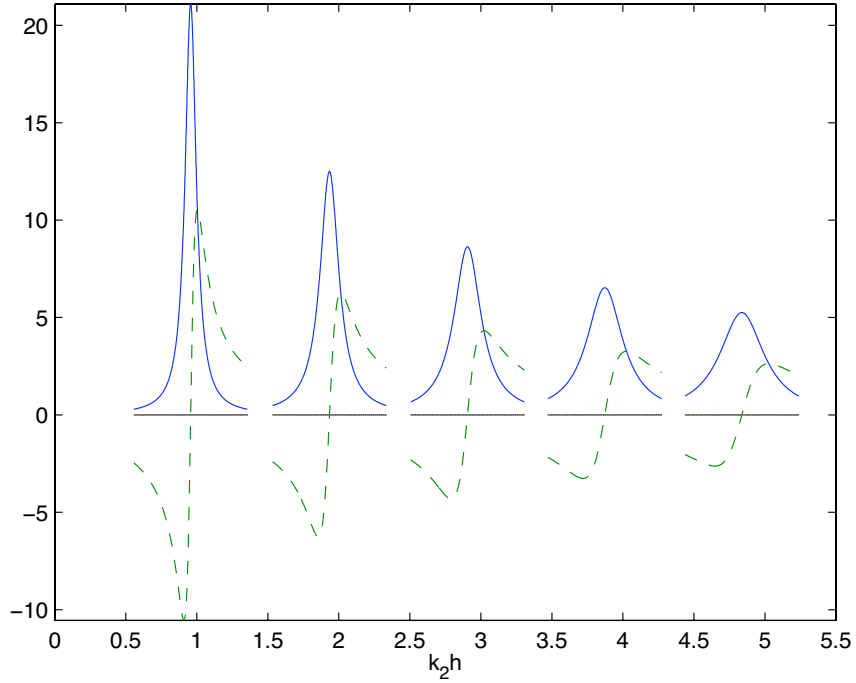


FIG. 1: Resonant scattering from wire; $\epsilon_r = 4$, $a/h = 10^{-4}$.

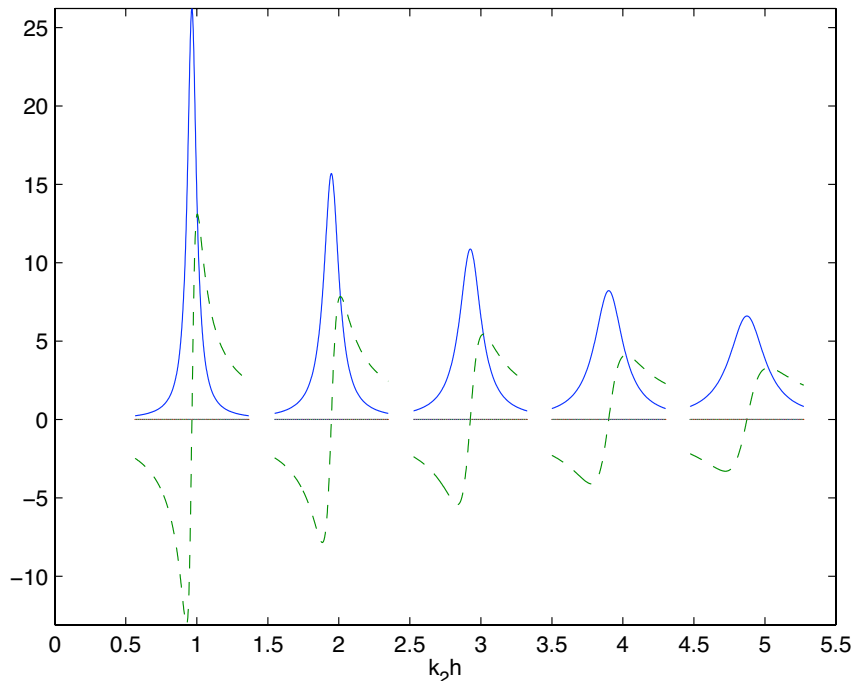


FIG. 2: Resonant scattering from wire; $\epsilon_r = 4$, $a/h = 10^{-5}$.

II. FORMULATION

The behavior of electromagnetic waves along and across the boundary between two media with different properties is much more complicated than the case of one homogeneous medium. Fortunately, this case of two media has been systematically studied [2]. The notations, approach, and results of this reference are to be used here.

For definiteness, let the two media be air and earth. Following the notation of Ref. [2], let the planar boundary between air and earth be in the xy -plane (i.e., $z = 0$) and the z -axis points in the direction of the earth. The problem of the strip antenna to be studied is shown schematically in Fig. 4. The length of the antenna is $2h$. Still following the notation of Ref. [2], let k_1 be the wave number of region 1 (earth) and k_2 that of region 2 (air). As holds for earth and air, it will be assumed throughout this report that

$$k_1 > k_2. \quad (2.1)$$

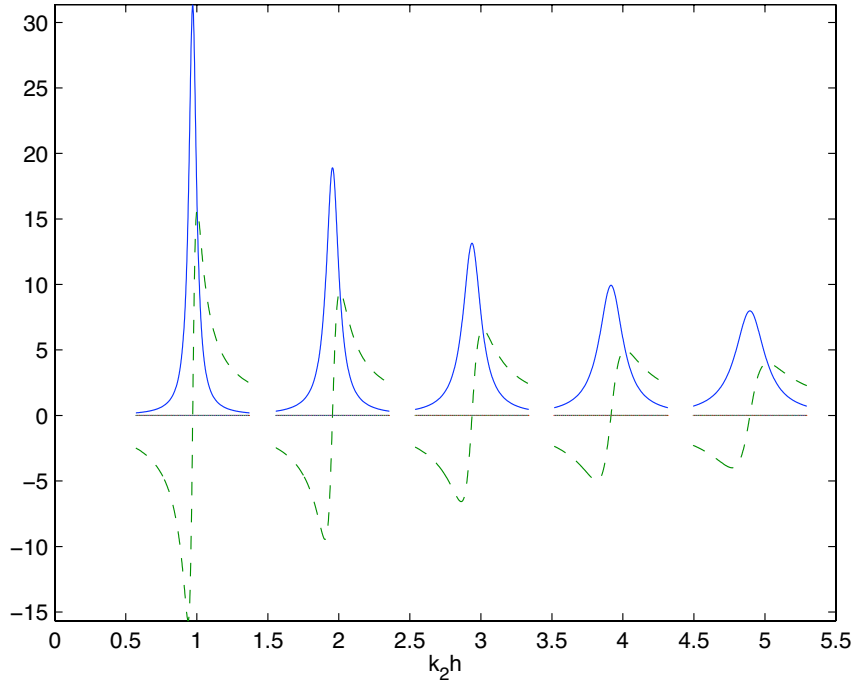


FIG. 3: Resonant scattering from wire; $\epsilon_r = 4$, $a/h = 10^{-6}$.

Since the antenna is assumed to be thin, a is taken to be small, so that

$$a \ll h \quad \text{and} \quad k_1 a \ll 1, \quad (2.2)$$

which, of course, implies $k_2 a \ll 1$. For present purposes both earth and air are assumed lossless, so that both k_1 and k_2 are taken to be real-valued and positive. As in the usual case of the linear antenna in a homogeneous medium, once the lossless case is understood, the introduction of loss in the medium is fairly straightforward.

The formulation of the problem hinges on the electric field generated by a “horizontal” point dipole in the interface. Consider a delta-function current at the origin,

$$\mathbf{J} = \delta(x) \delta(y) \delta(z) \hat{\mathbf{x}}; \quad (2.3)$$

then, the x -component of the electric field at a point $(x, y, 0)$ on the interface is given by (see Eq. (5.4.13) of Ref. [2])

$$E_x(x, y) = -\frac{\omega\mu_0}{4\pi^2} \int_{-\infty}^{\infty} d\xi \int_{-\infty}^{\infty} d\eta e^{i(\xi x + \eta y)} \frac{\gamma_1(k_2^2 - \xi^2) + \gamma_2(k_1^2 - \xi^2)}{MN}, \quad (2.4)$$

where

$$\begin{aligned}\gamma_1 &= (k_1^2 - \xi^2 - \eta^2)^{1/2}, & \gamma_2 &= (k_2^2 - \xi^2 - \eta^2)^{1/2}, \\ M &= \gamma_1 + \gamma_2, & N &= k_1^2 \gamma_2 + k_2^2 \gamma_1.\end{aligned}\tag{2.5}$$

In deriving Eq. (2.4), it has been assumed that the μ for both region 1 and region 2 is given by μ_0 ; that is, we do not deal here with magnetizable earth. Note that Eq. (2.4) does not change when the regions 1 and 2 are exchanged.

The advantage of studying a strip antenna of negligible thickness can be seen from Eq. (2.4). If the antenna is circular for example, then both the current source (2.3) and the observation point would have non-negligible values for the z -coordinate. In this case, the corresponding formula depends on the signs of these z coordinates and is much more complicated than the present Eq. (2.4).

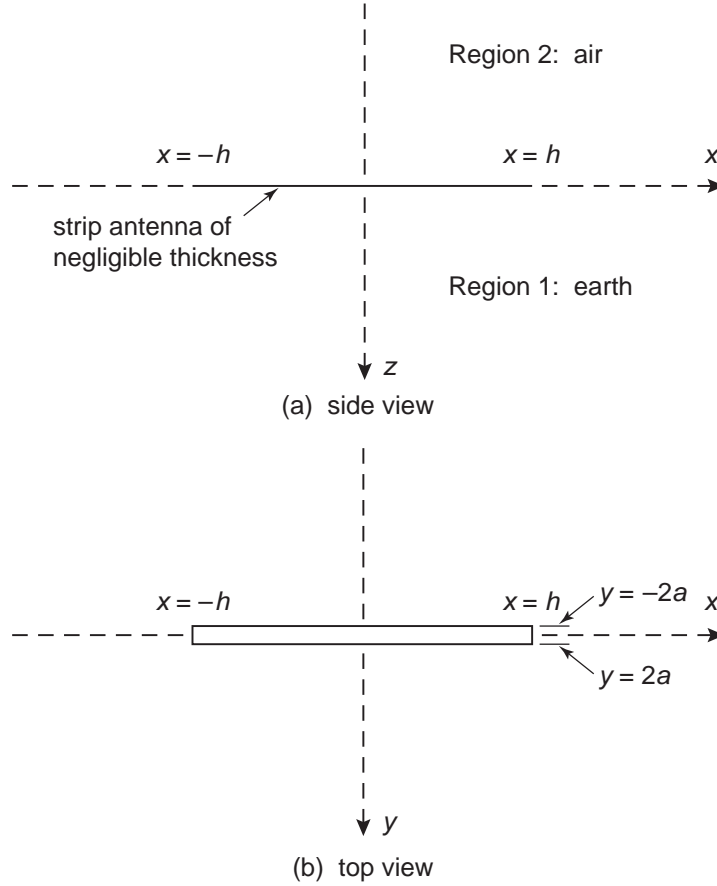


FIG. 4: Schematic diagram of the antenna geometry.

III. ZEROS IN THE FOURIER TRANSFORM OF E_x

The current induced in the strip will be shown to satisfy an integral equation of the Pocklington type. In the case of a single medium, as outlined in Appendix A, the kernel for the integral equation is derived easily once one notices a pair of zeros in the Fourier transform of E_x . That method works also for E_x for the case of a thin strip at an interface, except that one has to do some work to find the zeros. It is to this task that we now turn.

From Eq. (2.4) it follows that the Fourier transform from x to ξ of $E_x(x, y)$ is proportional to

$$\tilde{E}(\xi, y) \sim \int_{-\infty}^{\infty} d\eta e^{i\eta y} \frac{\gamma_1(k_2^2 - \xi^2) + \gamma_2(k_1^2 - \xi^2)}{MN}. \quad (3.1)$$

This $\tilde{E}(\xi, y)$ depends also on k_1 and k_2 , which in turn depend on frequency through

$$k_1 = \sqrt{\epsilon_1} \omega / c \quad \text{and} \quad k_2 = \sqrt{\epsilon_2} \omega / c, \quad (3.2)$$

where c is the speed of light and ϵ_1 and ϵ_2 are the relative dielectric constants of the two media (taking region 2 to be air, $k_2 \approx 1$). We assume lossless media, so that both ϵ_1 and ϵ_2 are real-valued and positive. In marked contrast to the case of a single medium, however, it will turn out that the zeros of $\tilde{E}(\xi, y)$ will be complex-valued. To proceed, we re-write Eq. (3.1) as

$$\tilde{E}(\xi, y) \sim -\xi^2 F_1(\xi, y) + F_2(\xi, y), \quad (3.3)$$

where

$$F_1(\xi, y) = \int_{-\infty}^{\infty} d\eta e^{i\eta y} \frac{1}{k_1^2 \gamma_2 + k_2^2 \gamma_1} \quad (3.4)$$

and

$$F_2(\xi, y) = \int_{-\infty}^{\infty} d\eta e^{i\eta y} \frac{1}{\gamma_1 + \gamma_2}. \quad (3.5)$$

Of these two functions, F_2 is the simpler one; in fact, it can be expressed exactly in terms of Bessel functions:

$$F_2(\xi, y) = \frac{\pi}{k_1^2 - k_2^2} \frac{1}{y} \left[\sqrt{k_1^2 - \xi^2} H_1^{(1)}(y \sqrt{k_1^2 - \xi^2}) - \sqrt{k_2^2 - \xi^2} H_1^{(1)}(y \sqrt{k_2^2 - \xi^2}) \right]. \quad (3.6)$$

Unfortunately, there does not seem to be a corresponding formula for F_1 . However, such an exact evaluation for F_1 is not needed. Since the thin antenna is by far the most important

case, as expressed by the condition $ka \ll 1$ of (2.2), there is a corresponding condition for this F_1 . Here y plays the role of a , because $|y| < 4a$. Taking y to be positive without loss of generality, the corresponding condition is

$$k_1 y \ll 1 \quad \text{and} \quad |\xi| y \ll 1. \quad (3.7)$$

An absolute value sign has been kept on ξ because, as to be seen later, ξ is allowed to be complex.

Before evaluating F_1 under condition (3.7), it is instructive to write down the corresponding approximate formula for the F_2 of Eq. (3.6). This is immediately

$$F_2(\xi, y) \sim \frac{\pi}{2} + i \left[\frac{(k_1^2 - \xi^2) \ln(y \sqrt{k_1^2 - \xi^2}) - (k_2^2 - \xi^2) \ln(y \sqrt{k_2^2 - \xi^2})}{k_1^2 - k_2^2} + \gamma - \ln 2 - \frac{1}{2} \right]. \quad (3.8)$$

Furthermore, from the series expansion for the Bessel function, the first neglected term is of the order of $(\bar{\xi} y)^2 |\ln(\bar{\xi} y)|$, where $\bar{\xi}$ is the larger one of k_1 and $|\xi|$. This point turns out to be of importance: what it means is that approximation (3.8) is highly accurate for small values of y .

The series expansion for this $F_2(\xi, y)$ is of the form

$$\ln(\bar{\xi} y), \quad 1, \quad (\bar{\xi} y)^2 \ln(\bar{\xi} y), \quad (\bar{\xi} y)^2, \quad (\bar{\xi} y)^4 \ln(\bar{\xi} y), \quad (\bar{\xi} y)^4, \quad \dots \quad (3.9)$$

for small values of y . As proved in Appendix B the corresponding series expansion for the $F_1(\xi, y)$ is also of the form (3.9). The task is therefore to determine the first two terms, namely those of orders $\ln(\bar{\xi} y)$ and 1, for $F_1(\xi, y)$ from Eq. (3.4).

As a first step in this direction, let $F_1(\xi, y)$ be written in the following form:

$$F_1(\xi, y) = \frac{-1}{k_1^2 - k_2^2} \int_{-\infty}^{\infty} d\eta e^{i\eta y} \frac{k_2^2 \sqrt{k_1^2 - \xi^2 - \eta^2} - k_1^2 \sqrt{k_2^2 - \xi^2 - \eta^2}}{k_1^2 k_2^2 - (k_1^2 + k_2^2)(\xi^2 + \eta^2)}. \quad (3.10)$$

The denominator here has a zero at

$$\xi^2 + \eta^2 = \frac{k_1^2 k_2^2}{k_1^2 + k_2^2}. \quad (3.11)$$

This is the famous Sommerfeld pole [3]. At this point, the numerator on the right-hand side of Eq. (3.10) also has a zero, implying the well-known fact that the Sommerfeld pole is on

the second sheet. From either Eq. (3.4) or Eq. (3.10), it is readily seen that the last factor in the integrand is of order η^{-1} for large values of η . Therefore, the leading term of order $\ln(\bar{\xi}y)$ for small values of y , as discussed in the preceding paragraph, comes from the integration over large values of η . It is thus desirable to separate out the part of the integrand that behaves as η^{-1} for large η ; in the rest of the terms, y can be simply put to zero. One way to accomplish this is to rewrite the right-hand side of Eq. (3.10) in the somewhat complicated form as follows:

$$F_1(\xi, y) = \frac{-1}{k_1^2 - k_2^2} \frac{1}{k_1^2 + k_2^2} \int_{-\infty}^{\infty} d\eta e^{i\eta y} \left[\frac{k_2^2}{\sqrt{k_1^2 - \xi^2 - \eta^2}} - \frac{k_1^2}{\sqrt{k_2^2 - \xi^2 - \eta^2}} \right. \\ \left. + \frac{k_1^2 k_2^2}{k_1^2 k_2^2 - (k_1^2 + k_2^2)(\xi^2 + \eta^2)} \left(\frac{k_1^2}{\sqrt{k_1^2 - \xi^2 - \eta^2}} - \frac{k_2^2}{\sqrt{k_2^2 - \xi^2 - \eta^2}} \right) \right]. \quad (3.12)$$

This way of rewriting Eq. (3.10) has several advantages. First, each of the four terms on the right-hand side contains either $\sqrt{k_1^2 - \xi^2 - \eta^2}$ or $\sqrt{k_2^2 - \xi^2 - \eta^2}$, but not both. Secondly, the first two integrations lead to Bessel functions. Thirdly, the quantity within the parentheses is zero at the Sommerfeld pole given by (3.11). Moreover, the integrand with this quantity as a factor decreases as η^{-3} for large η , and hence y can be put to zero in this integral, simplifying its evaluation greatly. These considerations lead to

$$F_1(\xi, y) \sim \frac{1}{k_1^2 + k_2^2} \left\{ \frac{\pi}{k_1^2 - k_2^2} \left[k_1^2 H_0^{(1)}(y\sqrt{k_2^2 - \xi^2}) - k_2^2 H_0^{(1)}(y\sqrt{k_1^2 - \xi^2}) \right] + F_{30} \right\}, \quad (3.13)$$

where

$$F_{30} = \frac{-1}{k_1^2 - k_2^2} \int_{-\infty}^{\infty} d\eta \frac{k_1^2 k_2^2}{k_1^2 k_2^2 - (k_1^2 + k_2^2)(\xi^2 + \eta^2)} \left(\frac{k_1^2}{\sqrt{k_1^2 - \xi^2 - \eta^2}} - \frac{k_2^2}{\sqrt{k_2^2 - \xi^2 - \eta^2}} \right) \quad (3.14)$$

is independent of y . Approximation (3.13) is accurate enough to give for F_1 the two leading terms of orders $\ln(\bar{\xi}y)$ and 1.

Since only these two leading terms are to be calculated, the Bessel functions on the right-hand side of Eq. (3.13) can be expanded to give

$$F_1(\xi, y) \sim \frac{1}{k_1^2 + k_2^2} \left[\pi + 2i \left(\frac{k_1^2 \ln(y\sqrt{k_2^2 - \xi^2}) - k_2^2 \ln(y\sqrt{k_1^2 - \xi^2})}{k_1^2 - k_2^2} + \gamma - \ln 2 \right) + F_{30} \right], \quad (3.15)$$

while a direct evaluation of Eq. (3.14) gives

$$F_{30} = -\frac{ik_1^2 k_2^2}{k_1^2 - k_2^2} \frac{1}{\sqrt{(k_1^2 + k_2^2)\xi^2 - k_1^2 k_2^2}} \times \left[\ln \frac{k_1^2 + \sqrt{(k_1^2 + k_2^2)\xi^2 - k_1^2 k_2^2}}{k_1^2 - \sqrt{(k_1^2 + k_2^2)\xi^2 - k_1^2 k_2^2}} - \ln \frac{k_2^2 + \sqrt{(k_1^2 + k_2^2)\xi^2 - k_1^2 k_2^2}}{k_2^2 - \sqrt{(k_1^2 + k_2^2)\xi^2 - k_1^2 k_2^2}} \right]. \quad (3.16)$$

Equation (3.16) has been written down for

$$\frac{k_1^2 k_2^2}{k_1^2 + k_2^2} < \xi^2 < k_2^2, \quad (3.17)$$

and analytic continuation can be used to ascertain the values of F_{30} outside this range of ξ^2 .

In summary, the substitution of (3.15), (3.16) and (3.8) into (3.3) gives explicitly

$$\begin{aligned} \tilde{E} \sim & \frac{\pi}{2} + i \left[\frac{(k_1^2 - \xi^2) \ln(y\sqrt{k_1^2 - \xi^2}) - (k_2^2 - \xi^2) \ln(y\sqrt{k_2^2 - \xi^2})}{k_1^2 - k_2^2} + \gamma - \ln 2 - \frac{1}{2} \right] \\ & - \frac{2\xi^2}{k_1^2 + k_2^2} \left\{ \frac{\pi}{2} + i \left[\frac{k_1^2 \ln(y\sqrt{k_2^2 - \xi^2}) - k_2^2 \ln(y\sqrt{k_1^2 - \xi^2})}{k_1^2 - k_2^2} + \gamma - \ln 2 \right] \right. \\ & - \frac{ik_1^2 k_2^2}{k_1^2 - k_2^2} \frac{1}{\sqrt{(k_1^2 + k_2^2)\xi^2 - k_1^2 k_2^2}} \\ & \left. \times \left[\ln \frac{k_1^2 + \sqrt{(k_1^2 + k_2^2)\xi^2 - k_1^2 k_2^2}}{\sqrt{k_1^2 - \xi^2}} - \ln \frac{k_2^2 + \sqrt{(k_1^2 + k_2^2)\xi^2 - k_1^2 k_2^2}}{\sqrt{k_2^2 - \xi^2}} \right] \right\}. \quad (3.18) \end{aligned}$$

This is the desired approximate expression from which to determine the zero of this \tilde{E} as a function of ξ when k_1 , k_2 and y are given subject to the conditions (3.7).

As a zeroth approximation, only the leading term of order $\ln(\bar{\xi}y)$ is kept while all terms of order 1 are neglected. In this approximation, the right-hand side of (3.18) is much simplified:

$$\tilde{E} \sim i \left(1 - \frac{2\xi^2}{k_1^2 + k_2^2} \right) \ln(\bar{\xi}y). \quad (3.19)$$

Thus, in this rough approximation, the zero of \tilde{E} , called k_0 , is given simply by

$$k_0^2 \approx \frac{k_1^2 + k_2^2}{2}. \quad (3.20)$$

What Eq. (3.20) means physically is as follows. Since this location k_0 of the zero of \tilde{E} is real, the current on a linear antenna at the planar boundary of two lossless dielectric

materials is approximately sinusoidal with a wave number given by $\sqrt{(k_1^2 + k_2^2)/2}$. This answers the two questions posed in the Introduction.

It must be remembered that (3.20) is only a rough approximation. It is the purpose of the remainder of this section to obtain a better approximation by taking into account not only the leading term of order $\ln(\bar{\xi}y)$ but also the next-to-leading term of order 1. Since the right-hand side of (3.18) is complex in the sense of having both a real part and an imaginary part, setting \tilde{E} to zero can be expected to lead to a solution ξ that is complex. Such a zero off the real axis leads to many new phenomena.

The zero-th order approximation (3.20) implies that, to this approximation,

$$\sqrt{k_1^2 - \xi^2} \sim \sqrt{\frac{k_1^2 - k_2^2}{2}} \quad \text{and} \quad \sqrt{k_2^2 - \xi^2} \sim \sqrt{-\frac{k_1^2 - k_2^2}{2}} = \sqrt{\frac{k_1^2 - k_2^2}{2}} e^{i\pi/2}. \quad (3.21)$$

On the basis of (3.21), define the dimensionless quantity

$$\bar{y} = y \sqrt{\frac{k_1^2 - k_2^2}{2}}, \quad (3.22)$$

and (3.18) takes the form

$$\begin{aligned} \tilde{E} \sim & i \frac{k_1^2 + k_2^2 - 2\xi^2}{k_1^2 + k_2^2} \left(\ln \bar{y} + \gamma - \ln 2 - \frac{i\pi}{2} \right) \\ & + i \left[\frac{(k_1^2 - \xi^2) \ln(\alpha \sqrt{k_1^2 - \xi^2}) - (k_2^2 - \xi^2) \ln(\alpha \sqrt{k_2^2 - \xi^2})}{k_1^2 - k_2^2} - \frac{1}{2} \right] \\ & - \frac{2i\xi^2}{k_1^2 + k_2^2} \left\{ \frac{k_1^2 \ln(\alpha \sqrt{k_2^2 - \xi^2}) - k_2^2 \ln(\alpha \sqrt{k_1^2 - \xi^2})}{k_1^2 - k_2^2} \right. \\ & - \frac{k_1^2 k_2^2}{k_1^2 - k_2^2} \frac{1}{\sqrt{(k_1^2 + k_2^2)\xi^2 - k_1^2 k_2^2}} \\ & \left. \times \left[\ln \frac{k_1^2 + \sqrt{(k_1^2 + k_2^2)\xi^2 - k_1^2 k_2^2}}{\sqrt{k_1^2 - \xi^2}} - \ln \frac{k_2^2 + \sqrt{(k_1^2 + k_2^2)\xi^2 - k_1^2 k_2^2}}{\sqrt{k_2^2 - \xi^2}} \right] \right\}, \quad (3.23) \end{aligned}$$

where

$$\alpha = \sqrt{\frac{2}{k_1^2 - k_2^2}}. \quad (3.24)$$

In (3.23), the small parameter \bar{y} appears only in the very first term. In the notation of (3.9), this first term is the only one of order $\ln(\bar{\xi}y)$, while everything else is of order 1.

It is curious to note that the α of Eq. (3.24) is infinity when $k_1 = k_2$, i.e., when the two media have the same electromagnetic properties. In this case, the zero of \tilde{E} is given *exactly* by $\xi = k_1 (= k_2)$, as already mentioned in Sec. III. Nevertheless, the case where k_1 and k_2 are close to each other requires a careful treatment. Since this case is not of great practical importance, it will be dealt with in Appendix C

The approximation (3.23) can be used to get a better approximation to the zero of \tilde{E} than that given by (3.20). A major reason to seek a better approximation is to find the imaginary part of this zero, including whether it remains zero. For this purpose, define

$$\tilde{E}^{(0)} = \tilde{E}(y) \Big|_{\xi^2 = (k_1^2 + k_2^2)/2}. \quad (3.25)$$

When (3.24) is used for $\tilde{E}(\xi, y)$, then this $\tilde{E}^{(0)}$ is independent of y .

It follows from (3.21) that

$$\ln(\alpha \sqrt{k_1^2 - \xi^2}) \Big|_{\xi^2 = (k_1^2 + k_2^2)/2} = 0 \quad \text{and} \quad \ln(\alpha \sqrt{k_2^2 - \xi^2}) \Big|_{\xi^2 = (k_1^2 + k_2^2)/2} = \frac{i\pi}{2}. \quad (3.26)$$

Accordingly, this $\tilde{E}^{(0)}$ is given by

$$\begin{aligned} \tilde{E}^{(0)} \sim & i \left[\frac{i\pi}{4} - \frac{1}{2} \right] - i \left\{ \frac{k_1^2}{k_1^2 - k_2^2} \frac{i\pi}{2} \right. \\ & \left. - \frac{k_1^2 k_2^2}{k_1^2 - k_2^2} \frac{1}{\sqrt{(k_1^4 + k_2^4)/2}} \left[\ln \frac{k_1^2 \sqrt{2} + \sqrt{k_1^4 + k_2^4}}{k_2^2 \sqrt{2} + \sqrt{k_1^4 + k_2^4}} + \frac{i\pi}{2} \right] \right\}. \end{aligned} \quad (3.27)$$

Note that this $\tilde{E}^{(0)}$ has both real and imaginary parts.

In terms of this $\tilde{E}^{(0)}$, the zero of $\tilde{E}(\xi, y)$ is given approximately by

$$k_0^2 \sim \frac{k_1^2 + k_2^2}{2} \left[1 - \frac{i\tilde{E}^{(0)}}{\ln(y\sqrt{(k_1^2 - k_2^2)/2}) + \gamma - \ln 2 - i\pi/2} \right]. \quad (3.28)$$

In the denominator, the terms $\gamma - \ln 2$ and $-i\pi/2$ may or may not be kept. Roughly speaking, it is the real part of $\tilde{E}^{(0)}$ that determines the imaginary part of the zero of $\tilde{E}(y)$.

Combining the real and imaginary parts separately, the $\tilde{E}^{(0)}$ as given in (3.9) can be rewritten as

$$\begin{aligned} \tilde{E}^{(0)} \sim & \frac{\pi}{2} \frac{1}{k_1^2 - k_2^2} \left[\frac{k_1^2 + k_2^2}{2} - \frac{k_1^2 k_2^2}{\sqrt{(k_1^4 + k_2^4)/2}} \right] \\ & - i \left[\frac{1}{2} - \frac{k_1^2 k_2^2}{k_1^2 - k_2^2} \frac{1}{\sqrt{(k_1^4 + k_2^4)/2}} \ln \frac{k_1^2 \sqrt{2} + \sqrt{k_1^4 + k_2^4}}{k_2^2 \sqrt{2} + \sqrt{k_1^4 + k_2^4}} \right]. \end{aligned} \quad (3.29)$$

TABLE 2: Sample values of the k_0^2/k_2^2 as a function of k_2a and k_1/k_2 .

k_2a	$k_1/k_2 = 1.8$	$k_1/k_2 = 2.0$	$k_1/k_2 = 2.2$
10^{-4}	$2.18318 + i0.12600$	$2.59013 + i0.16384$	$3.04044 + i0.20489$
10^{-5}	$2.16737 + i0.10080$	$2.56777 + i0.13092$	$3.01066 + i0.16348$
10^{-6}	$2.15777 + i0.08392$	$2.55413 + i0.10890$	$2.99250 + i0.13586$

For the real part, since

$$\sqrt{\frac{k_1^4 + k_2^4}{2}} \geq \frac{k_1^2 + k_2^2}{2},$$

it follows that

$$\frac{k_1^2 k_2^2}{\sqrt{(k_1^4 + k_2^4)/2}} \leq \frac{2k_1^2 k_2^2}{k_1^2 + k_2^2} \leq \frac{k_1^2 + k_2^2}{2},$$

and, hence, on the basis of (3.29),

$$\text{Re } \tilde{E}^{(0)} \geq 0 \tag{3.30}$$

with the equality sign only when $k_1 = k_2$. It is then a consequence of (3.28) that both the real and the imaginary parts of the zero of $\tilde{E}(\xi, y)$ in the ξ plane are positive when $k_1 > k_2$, at least for small values of y .

IV. INTEGRAL EQUATION FOR THE CURRENT

In the preceding section, the function $\tilde{E}(\xi, y)$, the Fourier transform of the electric field E_x except for an overall constant factor, is found to have a zero at $\xi = k_0$ say, where k_0 is given approximately by the square root (with positive real part) of the right-hand side of (3.28). That there is one and only one such k_0 plays a central role in formulating an integral equation for the current on the linear antenna at the boundary of two dielectric materials. Of course, $\xi = -k_0$ is also a zero of $\tilde{E}(\xi, y)$.

This k_0 has a number of important properties. First, as already mentioned, in the limiting case where $k_1 = k_2$, this k_0 is equal to k_1 . The details of how this limit is approached is to be found in Appendix C. In this limiting case, this $k_0 = k_1$ is essential in obtaining the

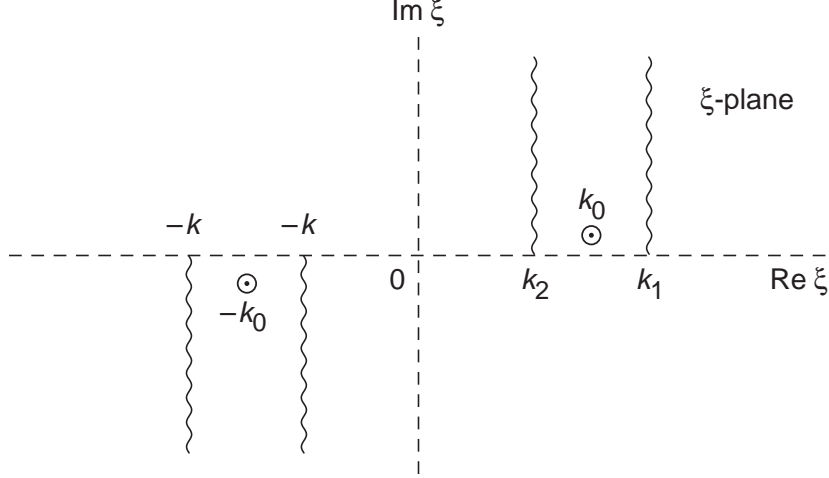


FIG. 5: A usual choice of the first sheet in the ξ -plane. With this and a number of similar choices, the zeros of $\tilde{E}(\xi, y)$ at $\xi = k_0$ and $\xi = -k_0$ are on the first sheet.

Hallén integral equation. Secondly, in the present, more general case of two media, this k_0 can be used in an analogous manner to give an integral equation for the current on the linear antenna. This is to be discussed in the remainder of this section. The importance of this k_0 is the underlying reason why it is studied in such detail in Sec. III. Thirdly, as seen from (3.30), this k_0 has a positive imaginary part. That k_0 is not real even in the absence of dissipation leads to features that are not seen in the usual case of the linear antenna in a uniform medium. Fourthly, this k_0 is in the first sheet of the complex ξ -plane as usually chosen—see Fig. 5. If this zero of $\tilde{E}(\xi, y)$ had been on the second sheet in a way similar to the Sommerfeld pole, the linear antenna on an interface would have qualitatively different properties. Define

$$\tilde{G}(\xi, y) = \frac{\tilde{E}(\xi, y)}{\xi^2 - k_0^2}. \quad (4.1)$$

Then, similar to $\tilde{E}(\xi, y)$, G is a function of k_1 , k_2 , ξ and y . It follows from (3.4) and (3.1) that

$$E_x = \frac{\omega\mu_0}{4\pi} \left(\frac{\partial^2}{\partial x^2} + k_0^2 \right) G(x, y), \quad (4.2)$$

where

$$G(x, y) = \int_{-\infty}^{\infty} d\xi e^{i\xi x} \tilde{G}(\xi, y) = \int_{-\infty}^{\infty} \frac{d\xi}{\xi^2 - k_0^2} \int_{-\infty}^{\infty} d\eta e^{i(\xi x + \eta y)} \frac{\gamma_1(k_2^2 - \xi^2) + \gamma_2(k_1^2 - \xi^2)}{MN} \quad (4.3)$$

is a function of k_1 , k_2 , x and y .

In order to gain some physical intuition for this G , consider once more the special case of $k_1 = k_2$, where this G simplifies to

$$G(x, y) = \frac{1}{2k_1^2} \int_{-\infty}^{\infty} d\xi \int_{-\infty}^{\infty} d\eta e^{i(\xi x + \eta y)} \frac{1}{\sqrt{k_1^2 - \xi^2 - \eta^2}}. \quad (4.4)$$

This integral can be easily evaluated using polar coordinates to give

$$G(x, y) = \frac{-\pi i}{k_1^2} \frac{e^{ik_1 \sqrt{x^2 + y^2}}}{\sqrt{x^2 + y^2}}. \quad (4.5)$$

Therefore, in this special case, G can be used to operate on the current to give the vector potential. In the present case of two media, although no vector potential can be usefully defined, this G of Eq. (4.4) plays the role of going from the current on the antenna to a “vector potential.” Thus G can be used to give an integral equation for the current.

At the beginning of Sec. II, it is noted that a thin strip antenna of width $4a$ is electromagnetically essentially the same as a circular one of radius a . Since the usual argument for this equivalence is not modified for the present, more general situation of two media, it will not be repeated here. This leads to the integro-differential equation

$$\left(\frac{\partial^2}{\partial x^2} + k_0^2 \right) \int_{-h}^h dx' \mathbf{K}(x - x') I(x') = \frac{4\pi}{\omega \mu_0} E_{\text{ap}}(x) \quad (4.6)$$

as a consequence of (4.2) and (4.3). Here the kernel \mathbf{K} of the equation is

$$\mathbf{K}(x) = \frac{1}{2\pi} \int_{-\pi}^{\pi} d\theta G(k_1, k_2, x, 2a \sin \frac{1}{2}\theta), \quad (4.7)$$

I is the current on the antenna, and $E_{\text{ap}}(x) \stackrel{\text{def}}{=} E_x^{\text{inc}}(x, 0)$ is the x -component of the external electric field applied to the thin strip, evaluated at $y = 0$.

Figure 6, obtained from the numerical work of Sec. VI and the appendices, shows the kernel $\mathbf{K}(x)$ for the case $k_1/k_2 = 2$ and $k_2 h = 5$, for two values of $a/h = 10^{-4}$ and $a/h = 10^{-6}$. Unlike the wire in a homogeneous medium, the kernels for the two cases of a/h differ noticeably even for values of $x \gg a$.

It is also of interest to compare the kernel $\mathbf{K}(x)$ for the case above with $a/h = 10^{-4}$ to the Hallén kernel in [1] for a single homogeneous medium adjusted to have a propagation

constant k_0 , and scaled to have the same limiting behavior as $\mathbf{K}(x)$ as x tends to zero. This Hallén kernel is

$$H(x) \stackrel{\text{def}}{=} -\frac{1}{(k_1 h)^2 + (k_2 h)^2} \int_0^{2\pi} d\theta \frac{\exp(ik_0 \sqrt{x^2 + 4a^2 \sin^2(\theta/2)})}{\sqrt{x^2 + 4a^2 \sin^2(\theta/2)}}. \quad (4.8)$$

Figure 7 compares $\mathbf{K}(x)$ against this $H(x)$ for the case $k_1/k_2 = 2$ and $k_2 h = 5$, with $a/h = 10^{-4}$.

V. METHOD OF DETERMINING RESONANCES

We believe that the resonant frequencies for scattering by a wire are relatively independent of the incident field, regardless of whether the wire is in a homogeneous medium or, as is the case here, at an interface. If there is no incident field, that is, if $E_{\text{ap}}(x) = 0$ on $-h \leq x \leq h$, then Eq. (4.6) specializes to

$$\left(\frac{\partial^2}{\partial x^2} + k_0^2 \right) \int_{-h}^h dx' \mathbf{K}(x - x') I(x') = 0. \quad (5.1)$$

At first glance, one might expect the only solution to be $I(x) = 0$. However, the key to defining resonance is to note that the kernel \mathbf{K} depends not only on position along the

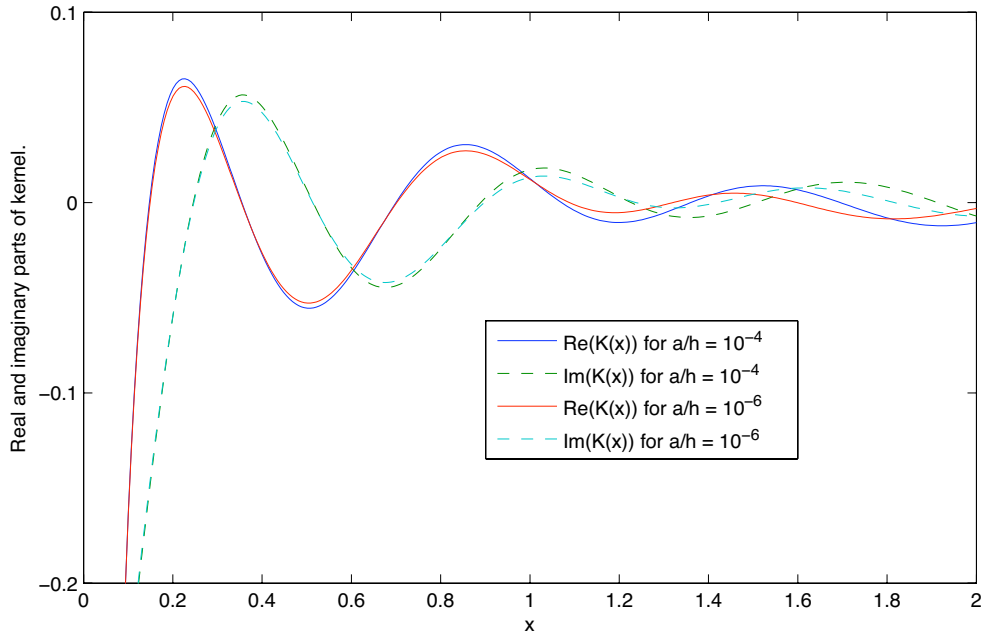


FIG. 6: Two cases of the kernel when $k_1/k_2 = 2$ and $k_2 h = 5$; $a/h = 10^{-4}$ and $a/h = 10^{-6}$.

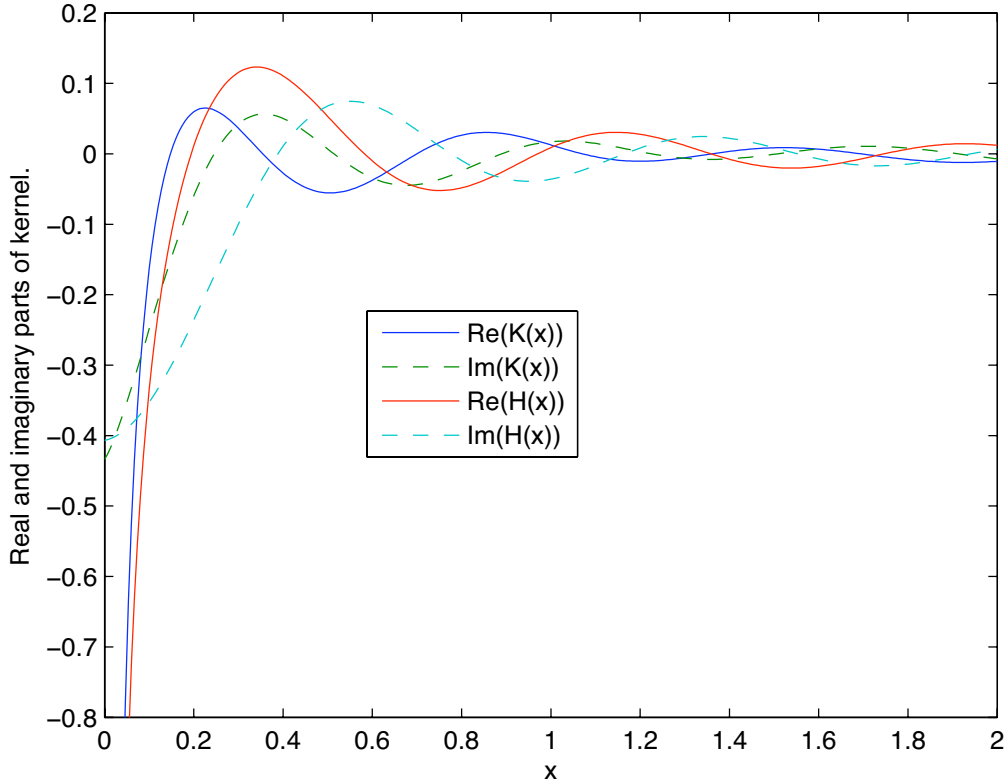


FIG. 7: Kernel $\mathbf{K}(x)$ compared with Hallén kernel $H(x)$ for case of $k_2 h = 5$, $k_1/k_2 = 2$, and $a/h = 10^{-4}$.

wire, but also on the angular frequency ω , on which k_1 and k_2 depend through Eq. (3.2). Therefore the solution to the integral equation (5.1) depends on ω and for certain discrete special values of ω , $\omega_1, \omega_2, \dots$, the equation has non-zero solutions. These values are expected to be complex, so that, listed in increasing order, we have

$$\begin{aligned} \text{Re } \omega_n &= \text{the } n\text{-th resonance frequency,} \\ -\text{Im } \omega_n &= \text{the width of the } n\text{-th resonance.} \end{aligned} \tag{5.2}$$

The real parts of the complex-valued solutions are the resonant frequencies, while the imaginary parts give the half-width at half height for each resonance, under the assumption that the resonant behavior for the n -th resonance is proportional to $1/(\omega - \omega_n)$. The task is to find the approximate values of the complex ω_n .

To determine the special frequencies, we use a Galerkin method, and for this we need to

symmetrize Eq. (4.6). For that, noting the boundary condition $I(\pm h) = 0$, we observe that

$$\begin{aligned}
\frac{\partial}{\partial x} \int_{-h}^h dx' \mathbf{K}(x-x') I(x') &= \int_{-h}^h dx' \left[\frac{\partial}{\partial x} \mathbf{K}(x-x') \right] I(x') \\
&= \int_{-h}^h dx' \left[-\frac{\partial}{\partial x'} \mathbf{K}(x-x') \right] I(x') \\
&= \int_{-h}^h dx' \left\{ -\frac{\partial}{\partial x'} [\mathbf{K}(x-x') I(x')] + \mathbf{K}(x-x') \left[\frac{\partial}{\partial x'} I(x') \right] \right\} \\
&= -\mathbf{K}(x-x') I(x') \Big|_{x'=-h}^{x'=h} + \int_{-h}^h dx' \mathbf{K}(x-x') \frac{\partial}{\partial x'} I(x') \\
&= \int_{-h}^h dx' \mathbf{K}(x-x') \frac{\partial}{\partial x'} I(x'). \tag{5.3}
\end{aligned}$$

With the use of this equation, Eq. (5.1) takes the symmetrical form

$$\frac{\partial}{\partial x} \int_{-h}^h dx' \mathbf{K}(x-x') \frac{\partial}{\partial x'} I(x') + k_0^2 \int_{-h}^h dx' \mathbf{K}(x-x') I(x') = 0. \tag{5.4}$$

This is the form of the Pocklington integral equation to which we shall apply Galerkin's method. We deal with the resonances that have symmetric currents separately from resonances for which the current is antisymmetric in x . For a trial current $I_{\text{Gal}}(x)$ in the Galerkin subspace, after an integration by parts Eq. (5.4) takes the approximate form:

$$\begin{aligned}
&\int_{-h}^h dx \left[-\frac{\partial}{\partial x} I_{\text{Gal}}(x) \right] \int_{-h}^h dx' \mathbf{K}(x-x') \frac{\partial}{\partial x'} I_{\text{Gal}}(x') \\
&+ k_0^2 \int_{-h}^h dx I_{\text{Gal}}(x) \int_{-h}^h dx' \mathbf{K}(x-x') I_{\text{Gal}}(x') = 0. \tag{5.5}
\end{aligned}$$

1. Galerkin subspace for resonances with symmetric and antisymmetric currents

For sufficiently small a , one expects resonant frequencies at complex values of k_0 near

$$\kappa_n \stackrel{\text{def}}{=} \frac{n\pi}{2h}, \tag{5.6}$$

for $n = 1, 2, \dots$, with the currents corresponding to odd values of n symmetric in x while the currents corresponding to even values of n are antisymmetric in x . In applying a Galerkin method, a critical question is this: should the Galerkin subspace depend on the frequency ω or not? For the symmetric case, there are good reasons to believe that the resonance current

is given roughly by the shifted cosine form $\cos kx - \cos kh$ [1]. One might expect to get a good approximation using a Galerkin subspace of dimension 1 by choosing the current to be the shifted-cosine; however, use of the shifted-cosine results in possibly spurious values of the resonant frequency. Examination of how these values arise shows that they are indeed spurious artifacts of the shifted-cosine form; hence we need to attend more carefully to the choice of the Galerkin subspace. The shifted-cosine form leads to a Galerkin subspace dependent on the frequency $\omega \sim k_2$. Question: should the Galerkin subspace depend on the frequency ω or not? Having encountered spurious values from the shifted-cosine form, we choose instead a Galerkin subspace that is *independent* of the frequency ω . This independence essentially determines the Galerkin subspace of dimension 1. To begin with, it can depend only on the geometric parameters h and a . Although we could force the Galerkin subspace to depend on a , we cannot see how to do this in a physically sensible way. Thus we take the Galerkin subspace to depend only on h . Then we can hardly avoid choosing $I_{\text{Gal}}^{\text{sym}}(x) \sim \cos \kappa_n x = \cos(n\pi x/2h)$ for the symmetric case where n is odd. Correspondingly, for the cases of resonance in which the current is antisymmetric about the center point of the wire, for which n is even, our Galerkin subspace consists of the single function $I_{\text{Gal}}^{\text{asym}} \sim \sin \kappa_n x$.

2. Resonances

With the chosen Galerkin subspace, Eq. (5.7) for the case of symmetric currents in which n is odd becomes

$$\begin{aligned} \int_{-h}^h dx \left[-\frac{\partial}{\partial x} \cos \kappa_n x \right] \int_{-h}^h dx' \mathbf{K}(x-x') \frac{\partial}{\partial x'} \cos \kappa_n x' \\ + k_0^2 \int_{-h}^h dx \cos \kappa_n x \int_{-h}^h dx' \mathbf{K}(x-x') \cos \kappa_n x' = 0. \end{aligned} \quad (5.7)$$

Note that the coefficient of the second term is k_0^2 rather than κ_n^2 . We define

$$I_{sn} \stackrel{\text{def}}{=} \int_{-h}^h dx \sin \kappa_n x \int_{-h}^h dx' \mathbf{K}(x-x') \sin \kappa_n x, \quad (5.8)$$

$$I_{cn} \stackrel{\text{def}}{=} \int_{-h}^h dx \cos \kappa_n x \int_{-h}^h dx' \mathbf{K}(x-x') \cos \kappa_n x, \quad (5.9)$$

and carry out the differentiations in Eq. (5.7) to obtain for n odd:

$$-\kappa_n^2 I_{sn} + k_0^2 I_{cn} = 0, \quad (5.10)$$

which in a form more convenient for calculation becomes,

$$(\kappa_n^2 - k_0^2)(I_{sn} + I_{cn}) + (\kappa_n^2 + k_0^2)(I_{sn} - I_{cn}) = 0; \quad (5.11)$$

Similarly for the resonances with antisymmetric currents so that n is even one finds:

$$\begin{aligned} \int_{-h}^h dx \left[-\frac{\partial}{\partial x} \sin \kappa_n x \right] \int_{-h}^h dx' \mathbf{K}(x - x') \frac{\partial}{\partial x'} \sin \kappa_n x' \\ + k^2 \int_{-h}^h dx \sin \kappa_n x \int_{-h}^h dx' \mathbf{K}(x - x') \sin \kappa_n x' = 0, \end{aligned} \quad (5.12)$$

which implies

$$(\kappa_n^2 - k_0^2)(I_{sn} + I_{cn}) - (\kappa_n^2 + k_0^2)(I_{sn} - I_{cn}) = 0, \quad (5.13)$$

We now make a zero-th order check. On replacing $\mathbf{K}(x - x')$ by a delta function $\delta(x - x')$ and carrying out the integrals in Eq. (5.7) and using the definition of $\kappa_n = (n\pi/2h)$, the result for n odd is $-\kappa_n^2 + k_0^2 = 0$; carrying out the same procedure on Eq. (5.12) yields this relation for n even; confirming our claim that for sufficiently small radius, the resonant propagation constants should be near κ_n .

Returning to deal with $\mathbf{K}(x - x')$ and not just the delta function, one holds fixed the geometrical and material parameters $h, a, \epsilon_1, \epsilon_2$ and μ_0 while varying the angular frequency ω in order to find complex values of ω for which Eq. (5.11) for the symmetric resonances and Eq. (5.13) for the antisymmetric resonances have non-zero solutions. Varying ω in the complex plane implies also varying the propagation constants k_1, k_2 via $k_j = \omega\sqrt{\epsilon_j}/c$ for $j = 1, 2$; and the dependence of k_1 and k_2 on (complex-valued) ω varies with k_0 as determined by Eq. (3.28).

The next step, derived in Appendix D, is to reduce the double integrals to single integrals to obtain, for all resonances, regardless of whether n is even or odd,

$$(\kappa_n^2 - k_0^2)I_{\Sigma n} = (\kappa_n^2 + k_0^2)I_{\Delta n}, \quad (5.14)$$

where we define

$$\begin{aligned} I_{\Sigma n} &\stackrel{\text{def}}{=} I_{sn} + I_{cn} = 2 \int_0^{2h} dx \mathbf{K}(x)(2h - x) \cos \kappa_n x, \\ I_{\Delta n} &\stackrel{\text{def}}{=} (-1)^n (I_{sn} - I_{cn}) = \frac{2}{\kappa_n} \int_0^{2h} dx \mathbf{K}(x) \sin \kappa_n x. \end{aligned} \quad (5.15)$$

3. Scaling to $h = 1$

For calculational purposes, we save effort by recognizing that the resonant frequencies scale with the wire half-length h . Thus one can set h to 1 and obtain resonant frequencies for other values of h by dividing by h . With $h = 1$ we have $\kappa_n = n\pi/2$ and the task is to solve the equation for resonances, namely, regardless of whether n is even or odd,

$$[(n\pi/2)^2 - k_0^2] I_{\Sigma n} = [(n\pi/2)^2 + k_0^2] I_{\Delta n}, \quad (5.16)$$

where with $h = 1$ and $\kappa_n = n\pi/2$ we have

$$\begin{aligned} I_{\Sigma n} &\stackrel{\text{def}}{=} I_{sn} + I_{cn} = 2 \int_0^2 dx \mathbf{K}(x)(2 - x) \cos \frac{n\pi x}{2}, \\ I_{\Delta n} &\stackrel{\text{def}}{=} (-1)^n (I_{sn} - I_{cn}) = \frac{4}{n\pi} \int_0^2 dx \mathbf{K}(x) \sin \frac{n\pi x}{2}. \end{aligned} \quad (5.17)$$

Similarly to the case of the wire in a homogeneous medium, when the strip width $4a$ is much smaller than all the other dimensions in this scattering problem, we can approximate the kernel $\mathbf{K}(x)$ (defined in Eq. (4.7)) by $G(x, a)$ defined in Eq. (4.3), so that we have

$$\mathbf{K}(x) \approx G(k_1, k_2, x, a) = \int_{-\infty}^{\infty} \frac{d\xi}{\xi^2 - k_0^2} \int_{-\infty}^{\infty} d\eta e^{i(\xi x + \eta a)} \frac{\gamma_1(k_2^2 - \xi^2) + \gamma_2(k_1^2 - \xi^2)}{MN}. \quad (5.18)$$

We will use this approximation to determine resonances.

VI. NUMERICAL ANALYSIS OF RESONANCES

Here we address the numerical analysis of Eqs. (5.16) through (5.18) for a wire scaled to a half-length of $h = 1$. Recall that k_0 is the zero of the Fourier transform of the kernel $\mathbf{K}(x)$. Later we will use the abbreviation

$$k_4 = k_1 k_2 / \sqrt{k_1^2 + k_2^2} = k_2 \sqrt{\frac{\epsilon}{\epsilon + 1}}, \quad (6.1)$$

so that for the relative dielectric constant ϵ real and positive, k_1 , k_2 , and k_4 as complex parameters all have the same argument.

For keeping track of branch cuts, in this section we study imaginary values of these parameters, and most of the following will deal in “kappa’s” and corresponding $\tilde{\gamma}$ ’s defined by

$$\text{(For } j = 0, 1, 2, 4) \quad k_j = i\kappa_j, \quad (6.2)$$

$$\text{(For } j = 1, 2) \quad \gamma_j = i\tilde{\gamma}_j, \quad (6.3)$$

where

$$\tilde{\gamma}_j \stackrel{\text{def}}{=} \sqrt{\xi^2 + \eta^2 + \kappa_j^2}. \quad (6.4)$$

For M and N defined in Eqs. (2.5) we have

$$M = i(\tilde{\gamma}_1 + \tilde{\gamma}_2), \quad \text{and} \quad N = -i(\kappa_2^2 \tilde{\gamma}_1^2 + \kappa_1^2 \tilde{\gamma}_2^2). \quad (6.5)$$

[**Note:** κ ’s as defined here have nothing to do with use of the κ_n symbol in the sections above.] The advantage to this notation is that for real κ ’s, the branch points and branch lines present no trouble. We then determine the proper branches involved in various integrals by following a path from positive real κ ’s to whatever complex values we want with the rule of “no cross branch lines” which tells us how to deform branch lines so as to avoid such crossings. Changing from k ’s to κ ’s and recognizing that numerical integration over the kernel $\mathbf{K}(x)$ takes almost a minute, we put Eq. (5.16) into the form

$$\int_0^2 dx \left\{ \left[\left(\frac{n\pi}{2} \right)^2 + \kappa_0^2 \right] (2-x) \cos \frac{n\pi x}{2} - \frac{2}{n\pi} \left[\left(\frac{n\pi}{2} \right)^2 - \kappa_0^2 \right] \sin \frac{n\pi x}{2} \right\} \mathbf{K}(x) = 0. \quad (6.6)$$

To express the kernel $\mathbf{K}(x)$ given in Eq. (5.18), we define

$$\tilde{M} \stackrel{\text{def}}{=} \tilde{\gamma}_1 + \tilde{\gamma}_2 \quad \text{and} \quad \tilde{N} = \kappa_2^2 \tilde{\gamma}_1 + \kappa_1^2 \tilde{\gamma}_2. \quad (6.7)$$

After dropping constants that cancel out in the equations above for resonant frequencies, for real-valued frequencies the kernel of the integral equation can be taken to be:

$$\mathbf{K}(x) = \int_{-\infty}^{\infty} \frac{d\xi}{\xi^2 + \kappa_0^2} \int_{-\infty}^{\infty} d\eta e^{i(\xi x + \eta a)} \frac{\tilde{\gamma}_1(\xi^2 + \kappa_2^2) + \tilde{\gamma}_2(\xi^2 + \kappa_1^2)}{(\tilde{\gamma}_1 + \tilde{\gamma}_2)(\kappa_2^2 \tilde{\gamma}_1 + \kappa_1^2 \tilde{\gamma}_2)}, \quad (6.8)$$

$$= \int_{-\infty}^{\infty} \frac{d\xi}{\xi^2 + \kappa_0^2} \int_{-\infty}^{\infty} d\eta e^{i(\xi x + \eta a)} \left(\frac{1}{\tilde{M}} + \frac{\xi^2}{\tilde{N}} \right). \quad (6.9)$$

Remark: for complex-valued resonant frequencies of interest, however, the integration path must be deformed to avoid crossing branch cuts. As a result the expressions to be developed for the kernel will be formulated in two steps: (1) in accordance with Eq. (6.9), and (2) by analytic continuation for the range of resonant frequencies that have positive real parts but negative imaginary parts, corresponding to $\kappa_2 = |\kappa_2|e^{-i\alpha}$ where α exceeds $\pi/2$.

The kernel $\mathbf{K}(x)$ depends on the resonant frequency through its dependence on κ_1 , κ_2 , and κ_0 , which itself is a function of κ_1 and κ_2 , provided by the MATLAB program `findk0A.m` in Appendix F.

The integrand has poles at $\xi = \pm i\kappa_0$. Adapting Eqs. (3.28) and (3.29) from k_0 to κ_0 , one shows that for a real-valued dielectric constant $\epsilon = 4$, over the range $0 \leq \alpha \leq 1.8$, $e^{i\alpha}\kappa_0$ has a relatively large positive real part and a small positive imaginary part. It is this pole that contributes in later work when we deform the integration path.

1. Summary of the kernel transformed for numerical calculation

The double integrals that define the kernel need to be put into a form that appears much more complicated but is more amenable to numerical work. Define

$$\mathcal{F}(u) \stackrel{\text{def}}{=} \frac{1}{u^3} \left[(1 + \kappa_2 u) e^{-\kappa_2 u} - (1 + \kappa_1 u) e^{-\kappa_1 u} \right]. \quad (6.10)$$

Then we find below that

$$\begin{aligned} \mathbf{K}(x) = & \frac{4\pi}{\kappa_1^4 - \kappa_2^4} \left\{ \mathcal{F}(\sqrt{x^2 + a^2}) \right. \\ & + \frac{2\kappa_0^2 - \kappa_1^2 - \kappa_2^2}{2\kappa_0^2} \int_0^x dx' \sinh \kappa_0(x - x') \mathcal{F}(\sqrt{x'^2 + a^2}) \left. \right\} \\ & + \mathbf{K}_2(0) \cosh \kappa_0 x + \mathbf{K}_{31}(x) + \mathbf{K}_{32}(x), \end{aligned} \quad (6.11)$$

where as shown in Appendix E,

$$\mathbf{K}_2(0) = \frac{\pi}{\kappa_1^2 - \kappa_2^2} \left(1 - \frac{2\kappa_0^2}{\kappa_1^2 + \kappa_2^2} \right) \left\{ \frac{2}{a} (e^{-\kappa_1 a} - e^{-\kappa_2 a}) \right.$$

$$\begin{aligned}
& + \frac{2}{\kappa_0 a} \left[\sqrt{\kappa_2^2 - \kappa_0^2} K_1 \left(a \sqrt{\kappa_2^2 - \kappa_0^2} \right) - \sqrt{\kappa_1^2 - \kappa_0^2} K_1 \left(a \sqrt{\kappa_1^2 - \kappa_0^2} \right) \right] \\
& + \kappa_1 - \kappa_2 + \frac{\kappa_2^2 - \kappa_0^2}{2\kappa_0} \ln \frac{\kappa_2 + \kappa_0}{\kappa_2 - \kappa_0} - \frac{\kappa_1^2 - \kappa_0^2}{2\kappa_0} \ln \frac{\kappa_1 + \kappa_0}{\kappa_1 - \kappa_0} \Big\} \quad (6.12)
\end{aligned}$$

$$\begin{aligned}
& \approx \frac{\pi}{\kappa_1^2 - \kappa_2^2} \left(1 - \frac{2\kappa_0^2}{\kappa_1^2 + \kappa_2^2} \right) \left[\kappa_2 - \kappa_1 - \frac{\kappa_1^2 - \kappa_2^2}{\kappa_0} \left(\ln \frac{a}{2} + \gamma - \frac{1}{2} \right) \right. \\
& \left. + \frac{\kappa_2^2 - \kappa_0^2}{\kappa_0} \ln(\kappa_2 + \kappa_0) - \frac{\kappa_1^2 - \kappa_0^2}{\kappa_0} \ln(\kappa_1 + \kappa_0) \right] + O(a^2 \ln a). \quad (6.13)
\end{aligned}$$

In the equation above, K_1 is a modified Bessel function [4]. For the remaining parts of the kernel we have

$$\begin{aligned}
\mathbf{K}_{31}(x) = & \frac{\pi}{\kappa_1^4 - \kappa_2^4} \left\{ \frac{2}{x} \left[\left(\kappa_0^2 - \kappa_2^2 + \frac{2\kappa_1}{x} + \frac{2}{x^2} \right) e^{-\kappa_1 x} \right. \right. \\
& \left. \left. - \left(\kappa_0^2 - \kappa_1^2 + \frac{2\kappa_2}{x} + \frac{2}{x^2} \right) e^{-\kappa_2 x} \right] - \kappa_0(\kappa_1^2 + \kappa_2^2 - \kappa_0^2) \left(\frac{\kappa_0}{\pi} T_{312}(x) \right) \right\} \\
& + \frac{\pi \kappa_0}{\kappa_1^2 + \kappa_2^2} e^{-\kappa_0 x}, \quad (6.14)
\end{aligned}$$

with

$$\begin{aligned}
\frac{\kappa_0}{\pi} T_{312}(x) = & e^{-\kappa_0 x} \left(\ln \frac{\kappa_1^2 - \kappa_0^2}{\kappa_0^2 - \kappa_2^2} + i\pi \right) + e^{-\kappa_0 x} (E_1[(\kappa_1 - \kappa_0)x] - E_1[(\kappa_2 - \kappa_0)x]) \\
& - e^{\kappa_0 x} (E_1[(\kappa_1 + \kappa_0)x] - E_1[(\kappa_2 + \kappa_0)x]); \\
\mathbf{K}_{32}(x) = & \frac{i\kappa_1 \kappa_2 \kappa_4}{\kappa_1^4 - \kappa_2^4} (G_2(x) - G_1(x)), \quad (6.15)
\end{aligned}$$

where for $j = 1, 2$ we define R_j by $R_1 \stackrel{\text{def}}{=} \kappa_1/\kappa_2$ and $R_2 \stackrel{\text{def}}{=} \kappa_2/\kappa_1$, and

$$\begin{aligned}
G_j(x) = & i\pi \kappa_0 e^{-\kappa_0 x} \frac{1}{\sqrt{\kappa_0^2 - \kappa_4^2}} \ln \frac{\sqrt{\kappa_0^2 - \kappa_4^2} - i\kappa_4 R_j}{\sqrt{\kappa_4^2 - \kappa_0^2} + i\kappa_4 R_j} \\
& - 2\pi i \int_0^{\sqrt{R_j^2 + 1} - 1} d\zeta \frac{(\zeta + 1)^2 \exp[-\kappa_4(\zeta + 1)x]}{[(\zeta + 1)^2 - \kappa_0^2/\kappa_4^2] \sqrt{\zeta(\zeta + 1)}}. \quad (6.16)
\end{aligned}$$

Note that the correct branch of the exponential integral $E_1[(\kappa_2 - \kappa_0)x]$ in the expression for $\mathbf{K}_{31}(x)$ requires adding $2\pi i$ in case the imaginary part of $\kappa_2 - \kappa_0$ is positive. Other important details concerning the branches of the above functions are given below. For $x < 0.001$ we make use of the relations

$$\begin{aligned} & \frac{2}{x} \left[\left(\kappa_0^2 - \kappa_2^2 + \frac{2\kappa_1}{x} + \frac{2}{x^2} \right) e^{-\kappa_1 x} - \left(\kappa_0^2 - \kappa_1^2 + \frac{2\kappa_2}{x} + \frac{2}{x^2} \right) e^{-\kappa_2 x} \right] \\ &= 2(\kappa_1 - \kappa_2) \left[\frac{2(\kappa_1^2 + \kappa_2^2) - \kappa_1 \kappa_2}{3} - \kappa_0^2 \right] + (\kappa_1^2 - \kappa_2^2) \left[\kappa_0^2 - \frac{\kappa_1^2 + \kappa_2^2}{2} \right] x + O(x^2), \end{aligned} \quad (6.17)$$

$$E_1(ax) - E_1(bx) = \log(b) - \log(a) + O(x^2). \quad (6.18)$$

Checks made on the correctness of these equations include the following: We checked that for $\alpha = \pi/2$ the kernel $\mathbf{K}(x)$ as computed here decreases toward zero for large values x ; this rules out any large error in $K_2(0)$. We checked that for a relative dielectric constant ϵ near 1, the computed kernel approaches the free-space case. We checked the $\mathbf{K}(x)$ varies smoothly, without jumps, as κ_0 is artificially scaled by a parameter that ranges from 0.3 to 1.1, and we checked that $\mathbf{K}(x)$ varies smoothly as α ranges from 0 to 2.

2. Putting the kernel in a form suitable for numerical analysis

We rearrange the integrand of Eq. (6.9) into three pieces in a way that makes it easy to calculate the piece most sharply peaked at $x = 0$

$$\frac{1}{\tilde{M}} + \frac{\xi^2}{\tilde{N}} = \frac{\xi^2 + \kappa_0^2}{\kappa_1^2 + \kappa_2^2} \frac{2}{\tilde{M}} + \left(1 - \frac{2\kappa_0^2}{\kappa_1^2 + \kappa_2^2} \right) \frac{1}{\tilde{M}} + \frac{\xi^2}{\kappa_1^2 + \kappa_2^2} \left(\frac{\kappa_1^2 + \kappa_2^2}{\tilde{N}} - \frac{2}{\tilde{M}} \right). \quad (6.19)$$

Correspondingly we have

$$\mathbf{K}(x) = \mathbf{K}_1(x) + \mathbf{K}_2(x) + \mathbf{K}_3(x), \quad (6.20)$$

where

$$\mathbf{K}_1(x) = \frac{2}{\kappa_1^2 + \kappa_2^2} \int_{-\infty}^{\infty} d\xi \int_{-\infty}^{\infty} d\eta e^{i(\xi x + \eta a)} \frac{1}{\tilde{M}}, \quad (6.21)$$

$$\mathbf{K}_2(x) = \left(1 - \frac{2\kappa_0^2}{\kappa_1^2 + \kappa_2^2} \right) \int_{-\infty}^{\infty} \frac{d\xi}{\xi^2 + \kappa_0^2} \int_{-\infty}^{\infty} d\eta e^{i(\xi x + \eta a)} \frac{1}{\tilde{M}}, \quad (6.22)$$

$$\begin{aligned} \mathbf{K}_3(x) &= \frac{1}{\kappa_1^2 + \kappa_2^2} \int_{-\infty}^{\infty} d\xi \frac{\xi^2}{\xi^2 + \kappa_0^2} \int_{-\infty}^{\infty} d\eta e^{i(\xi x + \eta a)} \left(\frac{\kappa_1^2 + \kappa_2^2}{\tilde{N}} - \frac{2}{\tilde{M}} \right) \\ &\approx \frac{1}{\kappa_1^2 + \kappa_2^2} \int_{-\infty}^{\infty} d\xi e^{i\xi x} \frac{\xi^2}{\xi^2 + \kappa_0^2} \int_{-\infty}^{\infty} d\eta \left(\frac{\kappa_1^2 + \kappa_2^2}{\tilde{N}} - \frac{2}{\tilde{M}} \right), \end{aligned} \quad (6.23)$$

where the last relation follows because the integrand falls off fast enough as η becomes large to make $\mathbf{K}_3(x)$ smooth as $x \rightarrow 0$, so that in the integrand we replace a by 0 without significant loss of accuracy. [Rechecked and found correct 18 July 2009.]

ACKNOWLEDGMENT

This work was undertaken at the suggestion of James Hersey, whom we thank for posing the problem and for many helpful discussions along the way.

APPENDIX A: COMPARISON WITH HOMOGENEOUS MEDIUM

In contrast to the assumption in the main report that $k_1 > k_2$, in this appendix we discuss the case $k_1 = k_2 = k$, for which Eq. (2.4) becomes

$$E_x(x, y) = -\frac{\omega\mu_0}{4\pi^2} \int_{-\infty}^{\infty} d\xi e^{i\xi x} \tilde{E}_x(\xi, y), \quad (\text{A1})$$

where

$$\tilde{E}_x(\xi, y) \stackrel{\text{def}}{=} (k^2 - \xi^2) \int_{-\infty}^{\infty} d\eta e^{i\eta y} \frac{1}{2k^2 \sqrt{k^2 - \xi^2 - \eta^2}} \quad (\text{A2})$$

is the Fourier transform from x to ξ of $E_x(x, y)$. From the factor $(k^2 - \xi^2)$ in $\tilde{E}_x(\xi, y)$ follows the relation for $E_x(x, y)$:

$$\begin{aligned} E_x(x, y) &= -\frac{\omega\mu_0}{4\pi^2} \left(\frac{d^2}{dx^2} + k^2 \right) \int_{-\infty}^{\infty} d\xi e^{i\xi x} \frac{\tilde{E}_x(\xi, y)}{k^2 - \xi^2} \\ &= -\frac{\omega\mu_0}{4\pi^2} \left(\frac{d^2}{dx^2} + k^2 \right) \int_{-\infty}^{\infty} d\xi \int_{-\infty}^{\infty} d\eta e^{i(\xi x + \eta y)} \frac{1}{2k^2 \sqrt{k^2 - \xi^2 - \eta^2}} \\ &= -\frac{\omega\mu_0}{4\pi^2} \left(\frac{d^2}{dx^2} + k^2 \right) G_0(x, y), \end{aligned} \quad (\text{A3})$$

where

$$G_0(x, y) = \frac{-\pi i}{k^2 \sqrt{x^2 + y^2}} e^{ik\sqrt{x^2 + y^2}}. \quad (\text{A4})$$

This G_0 generates the kernel of the integral equation of the Pocklington type for the current for the scattering by a thin perfectly conducting strip:

$$E^{\text{inc}}(x, y) = \frac{\omega\mu_0}{4\pi^2} \left(\frac{d^2}{dx^2} + k^2 \right) \int_{-\infty}^{\infty} dx' \int_{-2a}^{2a} dy' G(x - x', y - y') J_x(x', y'), \quad (\text{A5})$$

where by virtue of the slimness of the strip ($a \ll h$ and $ka \ll 1$), we ignore J_y , the current density transverse to the strip axis [1].

APPENDIX B: FORM OF SERIES EXPANSION FOR $F_1(\xi, y)$

In this appendix, a proof is given that, for small y , the series expansion for the $F_1(y) \equiv F_1(\xi, y)$ defined by Eq. (3.4) is of the form of (3.9), i.e.,

$$F_1(y) = \sum_{n=0}^{\infty} y^{2n} [a_n \ln y + a'_n]. \quad (\text{B1})$$

In view of the appearance of the logarithm, a Mellin transform should be used. Define

$$\tilde{F}_1(\zeta) = \int_0^{\infty} dy y^{-1+\zeta} F_1(y). \quad (\text{B2})$$

By Eq. (3.4), this is

$$\tilde{F}_1(\zeta) = 2 \int_0^{\infty} d\eta \frac{1}{k_1^2 \gamma_2 + k_2^2 \gamma_1} \int_0^{\infty} dy y^{-1+\zeta} \cos \eta y. \quad (\text{B3})$$

Since

$$\int_0^{\infty} dy y^{-1+\zeta} \cos \eta y = \eta^{-\zeta} 2^{\zeta-1} \sqrt{\pi} \frac{\Gamma\left(\frac{\zeta}{2}\right)}{\Gamma\left(\frac{1-\zeta}{2}\right)}, \quad (\text{B4})$$

Eq. (B3) reduces to

$$\tilde{F}_1(\zeta) = \sqrt{\pi} \frac{\Gamma\left(\frac{\zeta}{2}\right)}{\Gamma\left(\frac{1-\zeta}{2}\right)} \int_0^{\infty} d\eta \left(\frac{\eta}{2}\right)^{-\zeta} \frac{1}{k_1^2 \gamma_2 + k_2^2 \gamma_1}. \quad (\text{B5})$$

From the factor $\Gamma(\zeta/2)$, this $\tilde{F}_1(\zeta)$ has poles at negative even integer values (and zero) of ζ . Furthermore, for large η , $1/(k_1^2 \gamma_2 + k_2^2 \gamma_1)$ can be expanded into a series in odd powers of $1/\eta$. Using analytic continuation as usual in applying the method of the Mellin transform, the structure of this series leads to an additional factor of $1/(\zeta + 2n)$ near negative even integer values of ζ , but no such corresponding factor for negative odd integer values of ζ . This means that $\tilde{F}_1(\zeta)$ has double poles at negative even integer values of ζ , but is analytic at negative odd values of ζ . Therefore

$$\tilde{F}_1(\zeta) \sim \sum_{n=0}^{\infty} \left[\frac{-a_n}{(\zeta + 2n)^2} + \frac{a'_n}{\zeta + 2n} \right] \quad (\text{B6})$$

gives explicitly the positions and nature of the poles in the left half of the ζ -plane. The desired result Eq. (B1) follows from Eq. (B6) by inverting the Mellin transform (B2).

Note that we have paid no attention to the issue of whether the series on the right-hand side of Eq. (B1) is convergent or not. For the present purpose of studying the properties of a linear antenna on an interface, only the terms a_0 and a'_0 are of interest, and thus the convergence of the series is irrelevant.

APPENDIX C: CASE OF k_1 CLOSE TO k_2

In this appendix, the case in which k_1 and k_2 are close to each other is discussed.

When $k_1 = k_2$, the zero of \tilde{E} is given by $\xi = k_1 (= k_2)$. This limiting value is exact for all values of y . Nevertheless, only the case of small y as defined by (3.7) is to be treated. This special case corresponds to the wire on the interface being thin, and is especially simple to deal with, because the explicit results (3.28) and (3.29) of Sec. III can be used.

Since k_1 and k_2 are close to each other, it is convenient to define $\bar{k} > 0$ and $\epsilon > 0$ so that

$$k_1^2 = \bar{k}^2 + \epsilon^2 \quad \text{and} \quad k_2^2 = \bar{k}^2 - \epsilon^2. \quad (\text{C1})$$

With $\epsilon \ll \bar{k}$, various quantities are expanded in the small parameter ϵ^2/\bar{k}^2 .

Consider first the real part on the right-hand side of Eq. (3.29):

$$\frac{\pi}{2} \frac{1}{k_1^2 - k_2^2} \left[\frac{k_1^2 + k_2^2}{2} - \frac{k_1^2 k_2^2}{\sqrt{(k_1^4 + k_2^4)/2}} \right] = \frac{\pi}{2} \frac{1}{2\epsilon^2} \left[\bar{k}^2 - \frac{\bar{k}^4 - \epsilon^4}{\sqrt{\bar{k}^4 + \epsilon^4}} \right] \sim \frac{3\pi}{8} \frac{\epsilon^2}{\bar{k}^2}. \quad (\text{C2})$$

This is indeed positive, consistent with Eq. (3.30).

The imaginary part on the right-hand side of Eq. (3.29) can be treated in a similar way, only slightly more complicated:

$$\begin{aligned} & -\frac{1}{2} + \frac{k_1^2 k_2^2}{k_1^2 - k_2^2} \frac{1}{\sqrt{(k_1^4 + k_2^4)/2}} \ln \frac{k_1^2 \sqrt{2} + \sqrt{k_1^4 + k_2^4}}{k_2^2 \sqrt{2} + \sqrt{k_1^4 + k_2^4}} \\ & = -\frac{1}{2} + \frac{\bar{k}^4 - \epsilon^4}{2\epsilon^2} \frac{1}{\sqrt{\bar{k}^4 + \epsilon^4}} \ln \frac{\bar{k}^2 + \epsilon^2 + \sqrt{\bar{k}^4 + \epsilon^4}}{\bar{k}^2 - \epsilon^2 + \sqrt{\bar{k}^4 + \epsilon^4}} \\ & \sim -\frac{1}{2} + \frac{1}{2\epsilon^2} \left(\bar{k}^2 - \frac{3}{2} \frac{\epsilon^4}{\bar{k}^2} \right) \ln \frac{2\bar{k}^2 + \epsilon^2 + \frac{1}{2} \frac{\epsilon^4}{\bar{k}^2}}{2\bar{k}^2 - \epsilon^2 + \frac{1}{2} \frac{\epsilon^4}{\bar{k}^2}} \end{aligned}$$

$$\begin{aligned}
&\sim -\frac{1}{2} + \frac{1}{\epsilon^2} \left(\bar{k}^2 - \frac{3}{2} \frac{\epsilon^4}{\bar{k}^2} \right) \left[\frac{\epsilon^2}{2\bar{k}^2 + \frac{1}{2} \frac{\epsilon^4}{\bar{k}^2}} + \frac{1}{3} \left(\frac{\epsilon^2}{2\bar{k}^2} \right)^3 \right] \\
&\sim -\frac{1}{2} + \left(\bar{k}^2 - \frac{3}{2} \frac{\epsilon^4}{\bar{k}^2} \right) \left[\left(\frac{1}{2\bar{k}^2} - \frac{1}{8} \frac{\epsilon^4}{\bar{k}^6} \right) + \frac{1}{24} \frac{\epsilon^4}{\bar{k}^6} \right] \\
&\sim -\frac{7}{8} \frac{\epsilon^4}{\bar{k}^4}.
\end{aligned} \tag{C3}$$

In particular, this calculation shows the important role played by the first term, $-\frac{1}{2}$.

Finally, the substitution of Eqs. (C2) and (C3) into (3.28) gives the real and imaginary parts of ξ^2 , where ξ is the zero of $\tilde{E}(\xi, y)$:

$$\text{Re } \xi^2 \sim \bar{k}^2 - \frac{7}{8} \frac{\epsilon^4}{\bar{k}^2} \frac{1}{\ln(y\epsilon)} \tag{C4}$$

and

$$\text{Im } \xi^2 \sim -\frac{3\pi}{8} \frac{\epsilon^2}{\ln(y\epsilon)}, \tag{C5}$$

where the terms $\gamma - \ln 2 - i\pi/4$ in the denominator of Eq. (3.28) have been neglected because they are much smaller than $|\ln(y\epsilon)|$.

The results (C4) and (C5) are believed to be valid without the condition $k_1 y \ll 1$ of Eq. (3.7).

APPENDIX D: INTEGRATIONS FOR I_{cn} AND I_{sn}

Because $K(x - x')$ depends only on the difference between x and x' , it must be possible to rewrite the integrals

$$I_{sn} \stackrel{\text{def}}{=} \int_{-h}^h dx \sin \kappa_n x \int_{-h}^h dx' K(x - x') \sin \kappa_n x', \tag{D1}$$

$$I_{cn} \stackrel{\text{def}}{=} \int_{-h}^h dx \cos \kappa_n x \int_{-h}^h dx' K(x - x') \cos \kappa_n x \tag{D2}$$

as single integrals. We do this *without* using the fact that K is an even function of its argument. Define

$$I_e(\alpha, \alpha') = \int_{-h}^h dx e^{i\alpha x} \int_{-h}^h dx' K(x - x') e^{i\alpha' x'}. \tag{D3}$$

Changing integration variables $x \rightarrow -x'$ and $x' \rightarrow -x$ produces the relation

$$I_e(-\alpha', -\alpha) = I_e(\alpha, \alpha'). \quad (\text{D4})$$

With this relation one expresses I_{sn} and I_{cn} as

$$I_{sn} = -\frac{1}{4} [2I_e(\kappa_n, \kappa_n) - I_e(\kappa_n, -\kappa_n) - I_e(-\kappa_n, \kappa_n)], \quad (\text{D5})$$

$$I_{cn} = \frac{1}{4} [2I_e(\kappa_n, \kappa_n) + I_e(\kappa_n, -\kappa_n) + I_e(-\kappa_n, \kappa_n)], \quad (\text{D6})$$

so that we have

$$I_{sn} + I_{cn} = \frac{1}{2} [I_e(\kappa_n, -\kappa_n) + I_e(-\kappa_n, \kappa_n)], \quad (\text{D7})$$

$$I_{sn} - I_{cn} = -I_e(\kappa_n, \kappa_n). \quad (\text{D8})$$

For the reduction to single integrals we compute

$$\begin{aligned} I_e(\alpha, \alpha') &= \int_{-h}^h dx' \int_{-h}^h dx e^{i\alpha x} e^{i\alpha' x'} K(x - x') \\ &= \int_{-h}^h dx' \int_{-h-x'}^{h-x'} dy e^{i\alpha(y+x')} e^{i\alpha' x'} K(y) \\ &= \int_{-2h}^0 dy K(y) e^{i\alpha y} \int_{-h-y}^h dx' e^{i(\alpha+\alpha')x'} + \int_0^{2h} dy K(y) e^{i\alpha y} \int_{-h}^{h-y} dx' e^{i(\alpha+\alpha')x'} \\ &= \frac{1}{i(\alpha + \alpha')} \left[\int_{-2h}^0 dy K(y) e^{i\alpha y} \left(e^{i(\alpha+\alpha')h} - e^{-i(\alpha+\alpha')(h+y)} \right) \right. \\ &\quad \left. + \int_0^{2h} dy K(y) e^{i\alpha y} \left(e^{i(\alpha+\alpha')(h-y)} - e^{-i(\alpha+\alpha')h} \right) \right] \\ &= \frac{1}{i(\alpha + \alpha')} \left[\int_{-2h}^0 dy K(y) \left(e^{i(\alpha+\alpha')h} e^{i\alpha y} - e^{-i(\alpha+\alpha')h} e^{-i\alpha' y} \right) \right. \\ &\quad \left. + \int_0^{2h} dy K(y) \left(e^{i(\alpha+\alpha')h} e^{-i\alpha' y} - e^{-i(\alpha+\alpha')h} e^{i\alpha y} \right) \right]. \end{aligned} \quad (\text{D9})$$

The case $\alpha' = -\alpha$ is worked out directly to show

$$I_e(\alpha, -\alpha) = \int_{-2h}^0 dy K(y) (2h + y) e^{i\alpha y} + \int_0^{2h} dy K(y) (2h - y) e^{i\alpha y}. \quad (\text{D10})$$

Substitution of Eqs. (D9) and (D10) into Eqs. (D7) and (D8) yields

$$I_{sn} + I_{cn} = \int_{-2h}^0 dy K(y) (2h + y) \cos \kappa_n y + \int_0^{2h} dy K(y) (2h - y) \cos \kappa_n y, \quad (\text{D11})$$

$$I_{sn} - I_{cn} = -\frac{1}{\kappa_n} \left[\int_{-2h}^0 dy K(y) \sin[\kappa_n (2h + y)] + \int_0^{2h} dy K(y) \sin[\kappa_n (2h - y)] \right]. \quad (\text{D12})$$

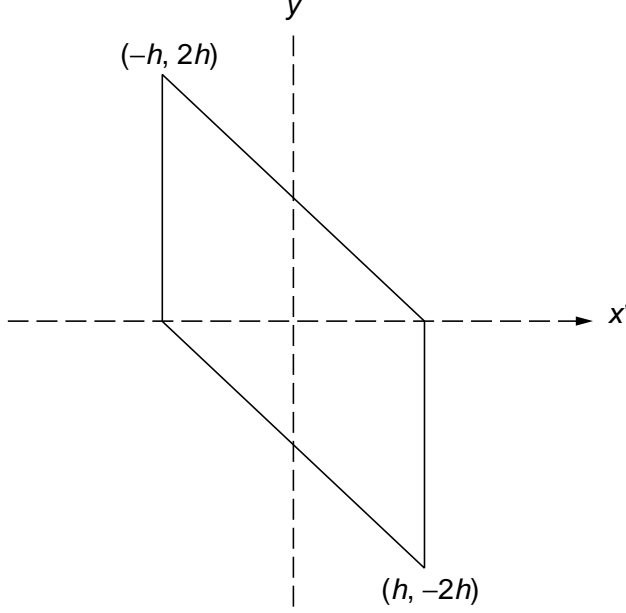


FIG. 8: Integration region on (x', y) -plane.

In the special case, which we have here, in which $K(y) = K(-y)$ and $\kappa_n = (n\pi/2h)$, these simplify to

$$\begin{aligned} I_{sn} + I_{cn} &= 2 \int_0^{2h} dy K(y) (2h - y) \cos \frac{n\pi y}{2h}, \\ I_{sn} - I_{cn} &= (-1)^n \frac{4h}{n\pi} \int_0^{2h} dy K(y) \sin \frac{n\pi y}{2h}, \end{aligned} \quad (\text{D13})$$

which are the single integrals that we wanted to obtain.

APPENDIX E: EVALUATION OF K_1 , K_2 , AND K_3

The integral in Eq. (6.21) that defines \mathbf{K}_1 is evaluated exactly as follows:

$$\mathbf{K}_1(x) = \frac{2}{\kappa_1^2 + \kappa_2^2} \int_{-\infty}^{\infty} d\xi \int_{-\infty}^{\infty} d\eta e^{i(\xi x + \eta a)} \frac{1}{\bar{M}} \quad (\text{E1})$$

$$= \frac{2}{\kappa_1^2 + \kappa_2^2} \int_{-\infty}^{\infty} d\xi \int_{-\infty}^{\infty} d\eta e^{i(\xi x + \eta a)} \frac{1}{\sqrt{\eta^2 + \xi^2 + k_1^2} + \sqrt{\eta^2 + \xi^2 + k_2^2}}. \quad (\text{E2})$$

Let

$$\rho \stackrel{\text{def}}{=} \sqrt{x^2 + a^2}, \quad (\text{E3})$$

and change to polar coordinates

$$x = \rho \cos \phi, \quad a = \rho \sin \phi, \quad \xi = \lambda \cos \alpha, \quad \text{and} \quad \eta = \lambda \sin \alpha, \quad (\text{E4})$$

leading to

$$\mathbf{K}_1(x) = \frac{2}{\kappa_1^2 + \kappa_2^2} \int_0^{2\pi} d\alpha \int_0^\infty \lambda d\lambda \frac{e^{i\rho\lambda \cos(\phi-\alpha)}}{\sqrt{\kappa_1^2 + \lambda^2} + \sqrt{\kappa_2^2 + \lambda^2}} \quad (\text{E5})$$

$$= \frac{4\pi}{\kappa_1^2 + \kappa_2^2} 2 \int_0^\infty \lambda d\lambda \frac{J_0(\lambda\rho)}{\sqrt{\kappa_1^2 + \lambda^2} + \sqrt{\kappa_2^2 + \lambda^2}} \quad (\text{E6})$$

$$= \frac{4\pi}{\kappa_1^4 - \kappa_2^4} [\mathcal{I}(\rho, \kappa_1) - \mathcal{I}(\rho, \kappa_2)], \quad (\text{E7})$$

where we define

$$\mathcal{I}(\rho, \kappa) \stackrel{\text{def}}{=} \int_0^\infty \lambda d\lambda J_0(\lambda\rho) \frac{\kappa^2 + \lambda^2}{\sqrt{\kappa^2 + \lambda^2}} \quad (\text{E8})$$

$$= \left(\kappa^2 - \frac{\partial^2}{\partial \rho^2} - \frac{1}{\rho} \frac{\partial}{\partial \rho} \right) \int_0^\infty \lambda d\lambda \frac{J_0(\lambda\rho)}{\sqrt{\kappa^2 + \lambda^2}} \quad (\text{E9})$$

$$= \left(\kappa^2 - \frac{\partial^2}{\partial \rho^2} - \frac{1}{\rho} \frac{\partial}{\partial \rho} \right) \frac{e^{-\kappa\rho}}{\rho} \quad (\text{E10})$$

$$= -\frac{1}{\rho^3} (1 + \kappa\rho) e^{-\kappa\rho}, \quad (\text{E11})$$

in which we used the relation $\left(\frac{\partial^2}{\partial \rho^2} + \frac{1}{\rho} \frac{\partial}{\partial \rho} + \lambda^2 \right) J_0(\lambda\rho) = 0$. Putting all this together yields

$$\mathbf{K}_1(x) = \frac{4\pi}{(\kappa_1^4 - \kappa_2^4)\rho^3} [(1 + \kappa_2\rho)e^{-\kappa_2\rho} - (1 + \kappa_1\rho)e^{-\kappa_1\rho}], \quad (\text{E12})$$

where x is related to ρ by Eq. (E3).

For $k_2\rho \ll 1$, it follows that

$$\mathbf{K}_1(x) = \frac{\pi}{\kappa_1^2 + \kappa_2^2} \left[\frac{2}{\rho} - \frac{4}{3} \frac{\kappa_1^2 + \kappa_1\kappa_2 + \kappa_2^2}{\kappa_1 + \kappa_2} + \frac{1}{2} (\kappa_1^2 + \kappa_2^2)\rho \right] + O(\rho^2). \quad (\text{E13})$$

1. Evaluation of $\mathbf{K}_2(x)$

From Eqs. (6.21) and (6.22) it follows that

$$\left(\kappa_0^2 - \frac{d^2}{dx^2} \right) \mathbf{K}_2(x) = \left(\frac{\kappa_1^2 + \kappa_2^2}{2} - \kappa_0^2 \right) \mathbf{K}_1(x). \quad (\text{E14})$$

Solving the differential equation and imposing the symmetry condition that $\mathbf{K}_2(x) = \mathbf{K}_2(-x)$ yield

$$\mathbf{K}_2(x) = \left(\kappa_0 - \frac{\kappa_1^2 + \kappa_2^2}{2\kappa_0} \right) \int_0^x dx' \sinh[\kappa_0(x - x')] \mathbf{K}_1(x') + \mathbf{K}_2(0) \cosh(\kappa_0 x). \quad (\text{E15})$$

The coefficient $\mathbf{K}_2(0)$ is a function of a which increases without bound as $a \rightarrow 0$; it is evaluated as follows (and implemented in `K20.m`). By the definition of \mathbf{K}_2 in Eq. (6.22),

$$\begin{aligned}
\mathbf{K}_2(0) &= \left(1 - \frac{2\kappa_0^2}{\kappa_1^2 + \kappa_2^2}\right) \int_{-\infty}^{\infty} \frac{d\xi}{\xi^2 + \kappa_0^2} \int_{-\infty}^{\infty} d\eta e^{i\eta a} \frac{1}{\tilde{\gamma}_1 + \tilde{\gamma}_2} \\
&= \frac{1}{\kappa_1^2 - \kappa_2^2} \left(1 - \frac{2\kappa_0^2}{\kappa_1^2 + \kappa_2^2}\right) \int_{-\infty}^{\infty} d\eta e^{i\eta a} \int_{-\infty}^{\infty} \frac{d\xi}{\xi^2 + \kappa_0^2} (\tilde{\gamma}_1 - \tilde{\gamma}_2) \\
&= \frac{1}{\kappa_1^2 - \kappa_2^2} \left(1 - \frac{2\kappa_0^2}{\kappa_1^2 + \kappa_2^2}\right) \left\{ \int_{-\infty}^{\infty} d\eta e^{i\eta a} \int_{-\infty}^{\infty} d\xi \left(\frac{1}{\tilde{\gamma}_1} - \frac{1}{\tilde{\gamma}_2} \right) \right. \\
&\quad \left. + \int_{-\infty}^{\infty} d\eta e^{i\eta a} \int_{-\infty}^{\infty} \frac{d\xi}{\xi^2 + \kappa_0^2} \left(\frac{\eta^2 + \kappa_1^2 - \kappa_0^2}{\tilde{\gamma}_1} - \frac{\eta^2 + \kappa_2^2 - \kappa_0^2}{\tilde{\gamma}_2} \right) \right\} \\
&= \frac{1}{\kappa_1^2 - \kappa_2^2} \left(1 - \frac{2\kappa_0^2}{\kappa_1^2 + \kappa_2^2}\right) (T_1 + T_2), \tag{E16}
\end{aligned}$$

where we define

$$T_1 \stackrel{\text{def}}{=} \int_{-\infty}^{\infty} d\eta e^{i\eta a} \int_{-\infty}^{\infty} d\xi \left(\frac{1}{\tilde{\gamma}_1} - \frac{1}{\tilde{\gamma}_2} \right) \tag{E17}$$

$$= \frac{2\pi}{a} (e^{-\kappa_1 a} - e^{-\kappa_2 a}) \approx -2\pi(\kappa_1 - \kappa_2), \tag{E18}$$

$$T_2 \stackrel{\text{def}}{=} \int_{-\infty}^{\infty} d\eta e^{i\eta a} [F_1(\eta) - F_2(\eta)], \tag{E19}$$

where for $j = 1, 2$ we define

$$F_j(\eta) \stackrel{\text{def}}{=} (\eta^2 + \kappa_j^2 - \kappa_0^2) \int_{-\infty}^{\infty} \frac{d\xi}{(\kappa_0^2 + \xi^2) \sqrt{\xi^2 + \eta^2 + \kappa_j^2}}, \tag{E20}$$

$$= \frac{i}{\kappa_0} \sqrt{\eta^2 + \kappa_j^2 - \kappa_0^2} \ln \left(\frac{\kappa_0 - i \sqrt{\eta^2 + \kappa_j^2 - \kappa_0^2}}{\kappa_0 + i \sqrt{\eta^2 + \kappa_j^2 - \kappa_0^2}} \right), \tag{E21}$$

$$= \frac{1}{\kappa_0} \sqrt{\eta^2 + \kappa_j^2 - \kappa_0^2} \left(\pi + i \ln \frac{\sqrt{\eta^2 + \kappa_j^2 - \kappa_0^2} + i \kappa_0}{\sqrt{\eta^2 + \kappa_j^2 - \kappa_0^2} - i \kappa_0} \right). \tag{E22}$$

The last form is convenient for obtaining the behavior for large $|\eta|$ [MATLAB check of Eq. (E21) against Eq. (E20) passed.] Thus we have

$$T_2 = T_{21} + T_{22}, \tag{E23}$$

where

$$T_{21} \stackrel{\text{def}}{=} \frac{\pi}{\kappa_0} \int_{-\infty}^{\infty} d\eta e^{i\eta a} \left(\sqrt{\eta^2 + \kappa_1^2 - \kappa_0^2} - \sqrt{\eta^2 + \kappa_2^2 - \kappa_0^2} \right), \quad (\text{E24})$$

$$= \frac{\pi}{\kappa_0} \int_{-\infty}^{\infty} d\eta e^{i\eta a} \left(\frac{\eta^2 + \kappa_1^2 - \kappa_0^2}{\sqrt{\eta^2 + \kappa_1^2 - \kappa_0^2}} - \frac{\eta^2 + \kappa_2^2 - \kappa_0^2}{\sqrt{\eta^2 + \kappa_2^2 - \kappa_0^2}} \right), \quad (\text{E25})$$

$$= \frac{\pi}{\kappa_0} \left[-\frac{d^2}{da^2} \int_{-\infty}^{\infty} d\eta e^{i\eta a} \left(\frac{1}{\sqrt{\eta^2 + \kappa_1^2 - \kappa_0^2}} - \frac{1}{\sqrt{\eta^2 + \kappa_2^2 - \kappa_0^2}} \right) \right. \\ \left. + \int_{-\infty}^{\infty} d\eta e^{i\eta a} \left(\frac{\kappa_1^2 - \kappa_0^2}{\sqrt{\eta^2 + \kappa_1^2 - \kappa_0^2}} - \frac{\kappa_2^2 - \kappa_0^2}{\sqrt{\eta^2 + \kappa_2^2 - \kappa_0^2}} \right) \right] \\ = T_{211} - T_{212}, \quad (\text{E26})$$

where

$$T_{21j} \stackrel{\text{def}}{=} \frac{\pi}{\kappa_0} \left(\kappa_j^2 - \kappa_0^2 - \frac{d^2}{da^2} \right) \int_{-\infty}^{\infty} \frac{d\eta e^{i\eta a}}{\sqrt{\eta^2 + \kappa_j^2 - \kappa_0^2}} \\ = \frac{2\pi}{\kappa_0} \left(\kappa_j^2 - \kappa_0^2 - \frac{d^2}{da^2} \right) K_0 \left(a \sqrt{\kappa_j^2 - \kappa_0^2} \right) \\ = -\frac{2\pi}{\kappa_0 a} \sqrt{\kappa_j^2 - \kappa_0^2} K_1 \left(a \sqrt{\kappa_j^2 - \kappa_0^2} \right), \quad (\text{E27})$$

$$= -\frac{2\pi}{\kappa_0} \left[\frac{1}{a^2} + \frac{\kappa_j^2 - \kappa_0^2}{2} \ln \frac{a \sqrt{\kappa_j^2 - \kappa_0^2}}{2} + \frac{1}{2} (\gamma - \frac{1}{2}) (\kappa_j^2 - \kappa_0^2) \right] \\ + O(a^2 \ln a). \quad (\text{E28})$$

(In the above equations, unlike the body of the paper, K_0 and K_1 denote modified Bessel functions [4].)

Equations (E26) and (E28) imply

$$T_{21} = \frac{2\pi}{\kappa_0 a} \left[\sqrt{\kappa_2^2 - \kappa_0^2} K_1 \left(a \sqrt{\kappa_2^2 - \kappa_0^2} \right) - \sqrt{\kappa_1^2 - \kappa_0^2} K_1 \left(a \sqrt{\kappa_1^2 - \kappa_0^2} \right) \right], \quad (\text{E29})$$

$$= -\frac{\pi}{\kappa_0} \left[(\kappa_1^2 - \kappa_0^2) \ln \frac{a \sqrt{\kappa_1^2 - \kappa_0^2}}{2} - (\kappa_2^2 - \kappa_0^2) \ln \frac{a \sqrt{\kappa_2^2 - \kappa_0^2}}{2} + (\gamma - \frac{1}{2}) (\kappa_1^2 - \kappa_2^2) \right] \\ + O(a^2 \ln a), \quad (\text{E30})$$

$$= -\frac{\pi}{\kappa_0} \left[(\kappa_1^2 - \kappa_2^2) \left(\ln \frac{a}{2} + \gamma - \frac{1}{2} \right) + \frac{\kappa_1^2 - \kappa_0^2}{2} \ln(\kappa_1^2 - \kappa_0^2) - \frac{\kappa_2^2 - \kappa_0^2}{2} \ln(\kappa_2^2 - \kappa_0^2) \right] \\ + O(a^2 \ln a). \quad (\text{E31})$$

(MATLAB checks OK.)

For T_{22} we have

$$\begin{aligned}
T_{22} &\stackrel{\text{def}}{=} \frac{i}{\kappa_0} \int_{-\infty}^{\infty} d\eta e^{i\eta a} \left[\sqrt{\eta^2 + \kappa_1^2 - \kappa_0^2} \ln \frac{\sqrt{\eta^2 + \kappa_1^2 - \kappa_0^2} + i\kappa_0}{\sqrt{\eta^2 + \kappa_1^2 - \kappa_0^2} - i\kappa_0} \right. \\
&\quad \left. - \sqrt{\eta^2 + \kappa_2^2 - \kappa_0^2} \ln \frac{\sqrt{\eta^2 + \kappa_2^2 - \kappa_0^2} + i\kappa_0}{\sqrt{\eta^2 + \kappa_2^2 - \kappa_0^2} - i\kappa_0} \right] \\
&= \frac{i}{\kappa_0} \int_{-\infty}^{\infty} d\eta \left[\sqrt{\eta^2 + \kappa_1^2 - \kappa_0^2} \ln \frac{\sqrt{\eta^2 + \kappa_1^2 - \kappa_0^2} + i\kappa_0}{\sqrt{\eta^2 + \kappa_1^2 - \kappa_0^2} - i\kappa_0} \right. \\
&\quad \left. - \sqrt{\eta^2 + \kappa_2^2 - \kappa_0^2} \ln \frac{\sqrt{\eta^2 + \kappa_2^2 - \kappa_0^2} + i\kappa_0}{\sqrt{\eta^2 + \kappa_2^2 - \kappa_0^2} - i\kappa_0} \right], \tag{E32}
\end{aligned}$$

$$= \pi \left(\kappa_1 - \kappa_2 + \frac{\kappa_2^2 - \kappa_0^2}{2\kappa_0} \ln \frac{\kappa_2 + \kappa_0}{\kappa_2 - \kappa_0} - \frac{\kappa_1^2 - \kappa_0^2}{2\kappa_0} \ln \frac{\kappa_1 + \kappa_0}{\kappa_1 - \kappa_0} \right), \tag{E33}$$

where the last expression is obtained to within an error of order $a^2 \ln a$ by the technique illustrated in Eq. (E78). That expression is implemented in the MATLAB routine `T22.m`. [May need to modify to deal with branch.]

Combining Eqs. (E31) and (E33) yields

$$\begin{aligned}
T_2 \approx \pi &\left[\kappa_1 - \kappa_2 - \frac{\kappa_1^2 - \kappa_2^2}{\kappa_0} \left(\ln \frac{a}{2} + \gamma - \frac{1}{2} \right) + \frac{\kappa_2^2 - \kappa_0^2}{\kappa_0} \ln(\kappa_2 + \kappa_0) \right. \\
&\quad \left. - \frac{\kappa_1^2 - \kappa_0^2}{\kappa_0} \ln(\kappa_1 + \kappa_0) \right]. \tag{E34}
\end{aligned}$$

2. Evaluation of K_3

From Eq. (6.23) we have

$$\mathbf{K}_3(x) \approx \frac{1}{\kappa_1^2 + \kappa_2^2} \int_{-\infty}^{\infty} d\xi e^{i\xi x} \frac{\xi^2}{\xi^2 + \kappa_0^2} \int_{-\infty}^{\infty} d\eta \left(\frac{\kappa_1^2 + \kappa_2^2}{\kappa_2^2 \tilde{\gamma}_1 + \kappa_1^2 \tilde{\gamma}_2} - \frac{2}{\tilde{\gamma}_1 + \tilde{\gamma}_2} \right). \tag{E35}$$

This can be rewritten as

$$\mathbf{K}_3(x) = \frac{2}{\kappa_1^2 + \kappa_2^2} \int_{-\infty}^{\infty} d\xi e^{i\xi x} F_3(\xi), \tag{E36}$$

where we define

$$F_3(\xi) = \frac{\xi^2}{\kappa_0^2 + \xi^2} \int_0^{\infty} d\eta \left(\frac{\kappa_1^2 + \kappa_2^2}{\kappa_2^2 \tilde{\gamma}_1 + \kappa_1^2 \tilde{\gamma}_2} - \frac{2}{\tilde{\gamma}_1 + \tilde{\gamma}_2} \right) \tag{E37}$$

$$= -\frac{\xi^2}{(\kappa_1^2 - \kappa_2^2)(\kappa_0^2 + \xi^2)} \int_0^\infty d\eta \left[2(\tilde{\gamma}_1 - \tilde{\gamma}_2) + \left(\eta^2 + \xi^2 + \frac{\kappa_1^2 \kappa_2^2}{\kappa_1^2 + \kappa_2^2} \right) \left(\frac{\kappa_2^2(\kappa_1^2 + \xi^2 + \eta^2)}{\tilde{\gamma}_1} - \frac{\kappa_1^2(\kappa_2^2 + \xi^2 + \eta^2)}{\tilde{\gamma}_2} \right) \right], \quad (\text{E38})$$

$$= -\frac{\xi^2}{(\kappa_1^2 - \kappa_2^2)(\kappa_0^2 + \xi^2)} \left[\frac{\kappa_1^2 - \kappa_2^2}{2} - \frac{\kappa_1^2 + \kappa_2^2 + \xi^2}{2} \log \frac{\kappa_1^2 + \xi^2}{\kappa_2^2 + \xi^2} + G(\kappa_1, \kappa_2, \xi) - G(\kappa_2, \kappa_1, \xi) \right]. \quad (\text{E39})$$

In (E39) we defined G by

$$G(\kappa_2, \kappa_1, \xi) \stackrel{\text{def}}{=} \kappa_1^2 \kappa_2^4 \int_0^\infty \frac{d\eta}{[(\kappa_1^2 + \kappa_2^2)(\eta^2 + \xi^2) + \kappa_1^2 \kappa_2^2] \sqrt{\eta^2 + \xi^2 + \kappa_2^2}}, \quad (\text{E40})$$

$$= \frac{i}{2} \frac{\kappa_1 \kappa_2 \kappa_4}{\sqrt{\xi^2 + \kappa_4^2}} \ln \frac{\sqrt{\xi^2 + \kappa_4^2} - i \kappa_4 \kappa_2 / \kappa_1}{\sqrt{\xi^2 + \kappa_4^2} + i \kappa_4 \kappa_2 / \kappa_1}, \quad (\text{E41})$$

where, as follows from Eq. (6.1),

$$\kappa_4 \stackrel{\text{def}}{=} \kappa_2 \sqrt{\epsilon / (\epsilon + 1)} = \frac{\kappa_1 \kappa_2}{\sqrt{\kappa_1^2 + \kappa_2^2}}. \quad (\text{E42})$$

Putting this together yields

$$\mathbf{K}_3(x) = \mathbf{K}_{31}(x) + \mathbf{K}_{32}(x), \quad (\text{E43})$$

where for $0 \leq \alpha < \pi/2$,

$$\mathbf{K}_{31}(x) = \frac{1}{\kappa_1^4 - \kappa_2^4} \int_{-\infty}^\infty d\xi \frac{e^{i\xi x} \xi^2}{\xi^2 + \kappa_0^2} \left[(\kappa_1^2 + \kappa_2^2 + \xi^2) \ln \frac{\kappa_1^2 + \xi^2}{\kappa_2^2 + \xi^2} - (\kappa_1^2 - \kappa_2^2) \right], \quad (\text{E44})$$

$$\begin{aligned} \mathbf{K}_{32}(x) &= i \frac{\kappa_1 \kappa_2 \kappa_4}{\kappa_1^4 - \kappa_2^4} \int_{-\infty}^\infty d\xi \frac{e^{i\xi x} \xi^2}{\xi^2 + \kappa_0^2} \frac{1}{\sqrt{\xi^2 + \kappa_4^2}} \\ &\times \left(\ln \frac{\sqrt{\xi^2 + \kappa_4^2} - i \kappa_4 \kappa_2 / \kappa_1}{\sqrt{\xi^2 + \kappa_4^2} + i \kappa_4 \kappa_2 / \kappa_1} - \ln \frac{\sqrt{\xi^2 + \kappa_4^2} - i \kappa_4 \kappa_1 / \kappa_2}{\sqrt{\xi^2 + \kappa_4^2} + i \kappa_4 \kappa_1 / \kappa_2} \right). \end{aligned} \quad (\text{E45})$$

3. Evaluation of the integral in \mathbf{K}_{31}

To evaluate the integral in Eq. (E44), we deform some contours and hence attend to branch points and branch cuts. As a first case consider a simplified integral, namely

$$\mathcal{J}_+ \stackrel{\text{def}}{=} \int_{-\infty}^\infty d\xi e^{i\xi x} \ln \frac{\xi - i}{\xi - 2i}, \quad (\text{E46})$$

under the condition that $x > 0$. The branch points are $\xi = i$ and $\xi = 2i$, both in the upper half ξ -plane. Avoid crossing branch lines by running the branch line up along the positive imaginary axis of the ξ -plane. Let $\xi - i = r_1 e^{i\phi_1}$ and $\xi - 2i = r_2 e^{i\phi_2}$, so we have

$$\frac{\xi - i}{\xi - 2i} = \frac{r_1}{r_2} e^{i(\phi_1 - \phi_2)}; \quad -\frac{3\pi}{2} < \phi_1, \phi_2 \leq \frac{\pi}{2}, \quad (\text{E47})$$

which implies

$$\ln \frac{\xi - i}{\xi - 2i} = \ln(r_1/r_2) + i(\phi_1 - \phi_2). \quad (\text{E48})$$

Deform the integration path to run from $i\infty - \epsilon$ down around $\xi = i$ and back up toward $i\infty + \epsilon$. Observe that in crossing the imaginary axis above $\text{Im } \xi = 2i$, there is no discontinuity in $\ln[(\xi - i)/(\xi - 2i)]$, so that above $\xi = 2i$, the contribution from the downward part of the path cancels the contribution from the upward part of the path. Therefore the path can be shrunk to a tight loop around the line segment connecting the two branch points. We have

$$(\forall \ 1 < w < 2) \quad \ln \frac{\xi - i}{\xi - 2i} \Big|_{\xi=iw+\epsilon} - \ln \frac{\xi - i}{\xi - 2i} \Big|_{\xi=iw-\epsilon} \xrightarrow{\epsilon \rightarrow 0} 0 - (-2\pi i) = 2\pi i, \quad (\text{E49})$$

whence it follows that

$$\mathcal{J}_+ = 2\pi i \int_1^2 i dw e^{-wx} = \frac{2\pi}{x} (e^{-2x} - e^{-x}). \quad (\text{E50})$$

Next observe that the integral with the branch points reflected about the real axis, so they are in the lower half ξ -plane, is

$$\mathcal{J}_- \stackrel{\text{def}}{=} \int_{-\infty}^{\infty} d\xi e^{i\xi x} \ln \frac{\xi + i}{\xi + 2i} = 0, \quad (\text{E51})$$

as follows from pushing the integration path infinitely upward. Thus Eq. (E50) gives us also the integral

$$\mathcal{J}_1 = \mathcal{J}_- + \mathcal{J}_+ = \int_{-\infty}^{\infty} d\xi e^{i\xi x} \ln \frac{\xi^2 + 1}{\xi^2 + 4} = \frac{2\pi}{x} (e^{-2x} - e^{-x}). \quad (\text{E52})$$

This procedure generalizes to produce

$$\mathcal{J}_1(x) \stackrel{\text{def}}{=} \int_{-\infty}^{\infty} d\xi e^{i\xi x} \ln \frac{\xi^2 + \kappa_1^2}{\xi^2 + \kappa_2^2} = \frac{2\pi}{|x|} (e^{-\kappa_2|x|} - e^{-\kappa_1|x|}). \quad (\text{E53})$$

[Checks OK in MATLAB.]

Now we evaluate the integrals in \mathbf{K}_{31} :

$$\mathbf{K}_{31}(x) = \frac{1}{\kappa_1^4 - \kappa_2^4} [(\kappa_1^2 + \kappa_2^2 - \kappa_0^2)(T_{311}(x) - \kappa_0^2 T_{312}(x)) + T_{314}(x)] + \frac{\kappa_0^2}{\kappa_1^2 + \kappa_2^2} T_{313}(x), \quad (\text{E54})$$

where

$$T_{311}(x) \stackrel{\text{def}}{=} \int_{-\infty}^{\infty} d\xi e^{i\xi x} \ln \frac{\xi^2 + \kappa_1^2}{\xi^2 + \kappa_2^2} = \mathcal{J}_1(x) = \frac{2\pi}{x} (e^{-\kappa_2 x} - e^{-\kappa_1 x}), \quad (\text{E55})$$

$$T_{312}(x) \stackrel{\text{def}}{=} \int_{-\infty}^{\infty} d\xi \frac{e^{i\xi x}}{\xi^2 + \kappa_0^2} \ln \frac{\xi^2 + \kappa_1^2}{\xi^2 + \kappa_2^2}, \quad (\text{E56})$$

$$T_{313}(x) \stackrel{\text{def}}{=} \int_{-\infty}^{\infty} d\xi \frac{e^{i\xi x}}{\xi^2 + \kappa_0^2} = \frac{\pi}{\kappa_0} e^{-\kappa_0 x}, \quad (\text{E57})$$

$$T_{314}(x) \stackrel{\text{def}}{=} \int_{-\infty}^{\infty} d\xi e^{i\xi x} \left(\xi^2 \ln \frac{\kappa_1^2 + \xi^2}{\kappa_2^2 + \xi^2} - \kappa_1^2 + \kappa_2^2 \right). \quad (\text{E58})$$

The integral $T_{312}(x)$ has two terms. From the pole at $\xi = i\kappa_0$ comes a term

$$\frac{\pi}{\kappa_0} e^{-\kappa_0 x} \ln \frac{\kappa_1^2 - \kappa_0^2}{\kappa_2^2 - \kappa_0^2} = \frac{\pi}{\kappa_0} e^{-\kappa_0 x} \left(\ln \frac{\kappa_1^2 - \kappa_0^2}{\kappa_0^2 - \kappa_2^2} + i\pi \right), \quad (\text{E59})$$

where the second expression comes from attending to the branch cut. The second term of $T_{312}(x)$ comes from a contour integral around the line segment connecting the branch points $i\kappa_2$ to $i\kappa_1$ so that for κ_2 such that branch crossings are no issue (that is, for $\alpha \leq \pi/2$ where $\arg \kappa_2 = -\alpha$) we have

$$T_{312}(x) = \frac{\pi}{\kappa_0} e^{-\kappa_0 x} \left(\ln \frac{\kappa_1^2 - \kappa_0^2}{\kappa_0^2 - \kappa_2^2} + i\pi \right) - 2\pi i \int_{i\kappa_2}^{i\kappa_1} d\xi \frac{e^{i\xi x}}{\xi^2 + \kappa_0^2}, \quad (\text{E60})$$

where

$$-2\pi i \int_{i\kappa_2}^{i\kappa_1} d\xi \frac{e^{i\xi x}}{\xi^2 + \kappa_0^2} = -\frac{\pi}{\kappa_0} \int_{i\kappa_2}^{i\kappa_1} d\xi e^{i\xi x} \left(\frac{1}{\xi - i\kappa_0} - \frac{1}{\xi + i\kappa_0} \right) \quad (\text{E61})$$

$$= \frac{\pi}{\kappa_0} \left\{ e^{-\kappa_0 x} (E_1[(\kappa_1 - \kappa_0)x] - E_1[(\kappa_2 - \kappa_0)x]) \right. \\ \left. - e^{\kappa_0 x} (E_1[(\kappa_1 + \kappa_0)x] - E_1[(\kappa_2 + \kappa_0)x]) \right\}. \quad (\text{E62})$$

Here E_1 is the exponential integral:

$$E_1(z) \stackrel{\text{def}}{=} \int_z^{\infty} dt \frac{e^{-t}}{t}. \quad (\text{E63})$$

(For small $|z|$, $E_1(z) = -\gamma - \ln z + z + O(z^2)$ where here γ is Euler's constant $\approx 0.5772\dots$)

As checked in MATLAB, the r.h.s of Eq. (E60) matches that of Eq. (E56) for values of α less than $\pi/2$; beyond that, Eq. (E60) gives the desired analytic continuation that would come from deforming the path in Eq. (E56) to avoid crossing branch lines.

The technique developed above shows that

$$T_{314}(x) = -2\pi i \int_{-i\kappa_2}^{i\kappa_1} d\xi \xi^2 e^{i\xi x}, \quad (\text{E64})$$

$$= 2\pi \left[\left(\frac{\kappa_1^2}{x} + \frac{2\kappa_1}{x^2} + \frac{2}{x^3} \right) e^{-\kappa_1 x} - \left(\frac{\kappa_2^2}{x} + \frac{2\kappa_2}{x^2} + \frac{2}{x^3} \right) e^{-\kappa_2 x} \right], \quad (\text{E65})$$

$$\rightarrow -\frac{2\pi}{3}(\kappa_1^3 - \kappa_2^3) + O(x) \quad \text{as } x \rightarrow 0. \quad (\text{E66})$$

Putting this together results in Eqs. (6.14) and (6.15).

Note that the correct branch of $E_1[(\kappa_2 - \kappa_0)x]$ requires adding $2\pi i$ in case the imaginary part of $\kappa_2 - \kappa_0$ is positive. This is done in MATLAB `mlab/branch/K31.m`, which exhibits smooth behavior over the range $0 \leq \alpha \leq 2$, as shown by `mlab/pltk3.m`.

4. Evaluation of $K_{32}(x)$

From Eq. (E45) we have

$$K_{32}(x) = \frac{i\kappa_1\kappa_2\kappa_4}{\kappa_1^4 - \kappa_2^4}(G_2 - G_1), \quad (\text{E67})$$

where we define R_j by $R_1 \stackrel{\text{def}}{=} \kappa_1/\kappa_2$ and $R_2 \stackrel{\text{def}}{=} \kappa_2/\kappa_1$ and

$$G_j \stackrel{\text{def}}{=} \int_{-\infty}^{\infty} d\xi \frac{e^{i\xi x} \xi^2}{\xi^2 + \kappa_0^2} \frac{1}{\sqrt{\xi^2 + \kappa_4^2}} \ln \frac{\sqrt{\xi^2 + \kappa_4^2} - i\kappa_4 R_j}{\sqrt{\xi^2 + \kappa_4^2} + i\kappa_4 R_j} \dots \quad (\text{E68})$$

Then for $j = 1, 2$, we split G_j into three terms:

$$G_j = G_{j0} + G_{j1} + G_{j2}, \quad (\text{E69})$$

in the following way. For G_j , $j = 1, 2$, deform the integration path as shown in Fig. 9, picking up a residue contribution G_{j0} at $\xi = i\kappa_0$, where the sign of κ_0 is determined as discussed in Appendix E 7. Then split integration path into two parts per diagram, one for G_{j1} around the line segment in the ξ -plane connecting $i\kappa_4$ and $i\kappa_j$; the other, G_{j2} , is from the U-shaped path vertically above κ_j .

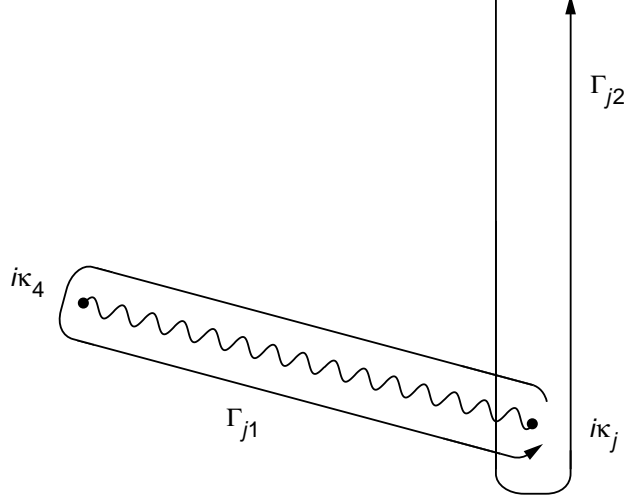


FIG. 9: Integration paths Γ_{j1} and Γ_{j2} on complex κ -plane.

[To test branch choices for the square root and the logarithm for G_{j2} , observe that the branch is easy to figure out for ξ having a large, positive imaginary part. To test the correctness of branch choices, we made a scatter plot on the complex plane of real and imaginary parts of the square-root involved and of the logarithmic term. If both of these scatter plots avoid branch lines and if the branch choice is correct in the limit of large positive imaginary part, we are in business. A neat thing about this procedure is that it works also when we change the integration variable for G_{j2} to y where $\xi = i(y + \kappa_j)$. This was done for enough values of $\arg \kappa_2$ and κ_0 to convince us that the branches are correct for the cases here.]

Using the technique discussed in Appendix E 5, we find $G_{j2} = 0$,

$$\begin{aligned} G_{j0} &= 2\pi i \frac{e^{-\kappa_0 x} (-\kappa_0^2)}{2i\kappa_0} \frac{1}{\sqrt{\kappa_4^2 - \kappa_0^2}} \ln \frac{\sqrt{\kappa_4^2 - \kappa_0^2} - i\kappa_4 R_j}{\sqrt{\kappa_4^2 - \kappa_0^2} + i\kappa_4 R_j} \\ &= -\pi\kappa_0 e^{-\kappa_0 x} \frac{1}{\sqrt{\kappa_4^2 - \kappa_0^2}} \ln \frac{\sqrt{\kappa_4^2 - \kappa_0^2} - i\kappa_4 R_j}{\sqrt{\kappa_4^2 - \kappa_0^2} + i\kappa_4 R_j} \end{aligned}$$

(and with the right choice of branch)

$$= i\pi\kappa_0 e^{-\kappa_0 x} \frac{1}{\sqrt{\kappa_0^2 - \kappa_4^2}} \ln \frac{\sqrt{\kappa_0^2 - \kappa_4^2} - i\kappa_4 R_j}{\sqrt{\kappa_0^2 - \kappa_4^2} + i\kappa_4 R_j}, \quad (\text{E70})$$

$$\begin{aligned} G_{j1} &= \int_{\Gamma_{j1}} d\xi \frac{e^{i\xi x} \xi^2}{\xi^2 + \kappa_0^2} \frac{1}{\sqrt{\xi^2 + \kappa_4^2}} \ln \frac{\sqrt{\xi^2 + \kappa_4^2} - i\kappa_4 R_j}{\sqrt{\xi^2 + \kappa_4^2} + i\kappa_4 R_j} \\ &= -2\pi i \int_0^{\sqrt{R_j^2 + 1} - 1} d\zeta \frac{(\zeta + 1)^2 \exp(-\kappa_4(\zeta + 1)x)}{[(\zeta + 1)^2 - \kappa_0^2/\kappa_4^2] \sqrt{\zeta(\zeta + 1)}}. \end{aligned} \quad (\text{E71})$$

In Eq. (E70) the square root has the branch cut as the negative real axis, and the square root of a positive number is positive. In Eq. (E71) ξ is related to the integration variable ζ by $\xi = i\kappa_4(\zeta + 1)$. The program that calculates G_j using these equations is `m1ab/Gj.m`. It has been tested against the defining equation over the range $0 \leq \alpha \leq 1.8$, and behaves smoothly (no branch jumps!) over that range. That program invokes as a subroutine `\kappa0h.m` to determine the appropriate value of κ_0 .

5. Study of a simplified integral relevant to G_j and to $K_2(0)$

Define

$$\mathcal{I} \stackrel{\text{def}}{=} \int_{-\infty}^{\infty} \frac{d\xi}{\sqrt{\xi^2 + 1}} \ln \frac{\sqrt{\xi^2 + 1} - i}{\sqrt{\xi^2 + 1} + i}. \quad (\text{E72})$$

By inspection, \mathcal{I} is purely imaginary. Deform the contour to come down the left side of the imaginary axis from $i\infty$ to i and back up the right side of the imaginary axis. Let $\xi = i(y + 1)$ to obtain

$$\mathcal{I} = \int_{\Gamma} \frac{dy}{\sqrt{y(y+2)}} \ln \frac{\sqrt{y(y+2)} - 1}{\sqrt{y(y+2)} + 1}, \quad (\text{E73})$$

where Γ runs from $\infty + i\delta$ to the origin of the y -plane and then down around the origin and back out to $\infty - i\delta$, so the branch line in the square root is the positive real axis. We require that the square root on the lower side of the branch line be ≥ 0 . From now on let $\sqrt{y(y+2)}$ denote the positive square root on the lower side of the branch line. Then, because the change in sign of the square root from above to below the branch line cancels the change in direction of the path above relative to the path below, we have

$$\begin{aligned} \mathcal{I} &= \int_0^{\infty} \frac{dy}{\sqrt{y(y+2)}} \left(\ln \frac{\sqrt{y(y+2)} - 1}{\sqrt{y(y+2)} + 1} + \ln \frac{-\sqrt{y(y+2)} - 1}{-\sqrt{y(y+2)} + 1} \right) \\ &= \int_0^{\infty} \frac{dy}{\sqrt{y(y+2)}} \left(\ln \frac{\sqrt{y(y+2)} - 1}{\sqrt{y(y+2)} + 1} + \ln \frac{\sqrt{y(y+2)} + 1}{\sqrt{y(y+2)} - 1} \right). \end{aligned} \quad (\text{E74})$$

Observe that $\sqrt{y(y+2)} - 1$ has a zero at $y = \sqrt{2} - 1$ which causes a singularity in the logarithms. Now observe also that

$$\ln \left(\sqrt{y(y+2)} - 1 \right) = \ln \left(1 - \sqrt{y(y+2)} \right) \pm i\pi. \quad (\text{E75})$$

Tracing the value of the square root on the chosen branch determines the sign, with the result that we find that the path splits into two pieces and that the path beyond the singular point at $y = \sqrt{2} - 1$ makes no contribution. The plus and minus signs for $i\pi$ turn out in such a way that we obtain

$$\mathcal{I} = -2\pi i \int_0^{\sqrt{2}-1} \frac{dy}{\sqrt{y(y+2)}} = \cosh^{-1}(\sqrt{2}). \quad (\text{E76})$$

This result is confirmed by a MATLAB integration.

6. Integral for $K_2(0)$

The same line of reasoning shows the relation

$$\int_{-\infty}^{\infty} d\xi e^{i\xi a} \left[\sqrt{\xi^2 + 1} \ln \frac{\sqrt{\xi^2 + 1} - i}{\sqrt{\xi^2 + 1} + i} + 2i \right] = 2\pi i \int_0^{\sqrt{2}-1} dy e^{-(y+1)a} \sqrt{y(y+2)}, \quad (\text{E77})$$

which for the special case of $a \rightarrow 0$ yields

$$\begin{aligned} \int_{-\infty}^{\infty} d\xi \left(\sqrt{\xi^2 + 1} \ln \frac{\sqrt{\xi^2 + 1} + ib}{\sqrt{\xi^2 + 1} - ib} - 2ib \right) &= -2i\pi \int_1^{\sqrt{1+b^2}} dt \sqrt{t^2 - 1} \\ &= i\pi \left[\ln \left(b + \sqrt{1+b^2} \right) - b\sqrt{1+b^2} \right]. \end{aligned} \quad (\text{E78})$$

[Eq. (E78) checks correct in MATLAB.]

7. Pole for residue contribution to G_j

The equation for the parameter κ_0 , the location of the pole in the Fourier transform of the kernel, determines only κ_0^2 . In the defining equations for the kernel κ_0 enters only as κ_0^2 , so the sign of κ_0 does not matter; however, in performing contour integrals a residue from only one of the two poles in the ξ -plane at $\xi = \pm\kappa_0$ contributes, so that the sign of κ_0 matters. For the path deformations considered, the pole that contributes is that specified in the remark under Eq. (6.9)

8. Evaluating zeros in Fourier transform of electric-field kernel

To evaluate Eq. (3.3) in cases of complex-valued propagation constants and with y set equal to a , we use the “kappa’s” to put Eq. (3.3) in the form

$$\tilde{E}(\xi, a) \sim -\xi^2 F_1(a, \xi) + F_2(a, \xi), \quad (\text{E79})$$

where, now using “kappa’s” we have

$$F_1(a, \xi) \stackrel{\text{def}}{=} i \int_{-\infty}^{\infty} d\eta e^{i\eta a} \frac{1}{\kappa_1^2 \tilde{\gamma}_2 + \kappa_2^2 \tilde{\gamma}_1}, \quad (\text{E80})$$

$$F_2(a, \xi) \stackrel{\text{def}}{=} -i \int_{-\infty}^{\infty} d\eta e^{i\eta a} \frac{1}{\tilde{\gamma}_1 + \tilde{\gamma}_2}. \quad (\text{E81})$$

Thus we seek the values of ξ , denoted ξ_0 for which, copying Eq. (3.3),

$$0 = -\xi^2 F_1(\xi, a) + F_2(\xi, a), \quad (\text{E82})$$

where in terms of “kappa’s” we have

$$\begin{aligned} F_1(\xi, a) = & \frac{i}{\kappa_1^2 + \kappa_2^2} \left\{ \frac{1}{\kappa_1^2 - \kappa_2^2} \left[\kappa_1^2 \ln \frac{\xi^2 + 2\kappa_4^2}{\xi^2 + \kappa_2^2} - \kappa_2^2 \ln \frac{\xi^2 + 2\kappa_4^2}{\xi^2 + \kappa_1^2} \right. \right. \\ & - 2G(\kappa_1, \kappa_2, \xi) + 2G(\kappa_2, \kappa_1, \xi) \Big] \\ & \left. + 2K_0 \left(a \sqrt{\xi^2 + 2\kappa_4^2} \right) \right\} + O(u^4 \ln u), \end{aligned} \quad (\text{E83})$$

where $u = |a|(\kappa + |\xi|)$, with $\kappa = \max(|\kappa_1|, |\kappa_2|)$ and we recall that $\kappa_4 \stackrel{\text{def}}{=} \kappa_2 \sqrt{\epsilon/(\epsilon + 1)}$ so that $\kappa_4^2 = \frac{\kappa_1^2 \kappa_2^2}{\kappa_1^2 + \kappa_2^2}$, and $G(\kappa_2, \kappa_1, \xi)$ is the function defined in Eq. (E41).

Putting all this together and dropping terms $O(u^2 \ln u)$ gives

$$\begin{aligned} F_1(\xi, a) = & \frac{i}{\kappa_1^2 + \kappa_2^2} \left[2 \left(\ln \frac{2}{a} - \gamma \right) + \frac{\kappa_2^2 \ln(\xi^2 + \kappa_1^2) - \kappa_1^2 \ln(\xi^2 + \kappa_2^2)}{\kappa_1^2 - \kappa_2^2} \right. \\ & \left. + \frac{i\kappa_1 \kappa_2 \kappa_4}{(\kappa_1^2 - \kappa_2^2) \sqrt{\xi^2 + \kappa_4^2}} \left(\ln \frac{\sqrt{\xi^2 + \kappa_4^2} - \frac{i\kappa_2 \kappa_4}{\kappa_1}}{\sqrt{\xi^2 + \kappa_4^2} + \frac{i\kappa_2 \kappa_4}{\kappa_1}} - \ln \frac{\sqrt{\xi^2 + \kappa_4^2} - \frac{i\kappa_1 \kappa_4}{\kappa_2}}{\sqrt{\xi^2 + \kappa_4^2} + \frac{i\kappa_1 \kappa_4}{\kappa_2}} \right) \right]. \end{aligned} \quad (\text{E84})$$

For numerical evaluation, we note that the zeros in the ξ -plane are near $\xi_0 = \pm i\kappa_2 \sqrt{(\epsilon + 1)/2} e^{i\delta}$ where δ is small and positive.

We also find analytically (and checked numerically):

$$F_2(\xi, a) = \frac{-i}{\kappa_1^2 - \kappa_2^2} \int_{-\infty}^{\infty} d\eta e^{i\eta a} (\tilde{\gamma}_1 - \tilde{\gamma}_2), \quad (\text{E85})$$

$$= \frac{-2i}{\kappa_1^2 - \kappa_2^2} \sum_{j=1}^2 (-1)^j \frac{1}{a} \sqrt{\kappa_j^2 + \xi^2} K_1 \left(a \sqrt{\kappa_j^2 + \xi^2} \right). \quad (\text{E86})$$

The small-argument approximation for the modified Bessel function K_1 (from [4], p. 9 and [5], p. 15 for ψ -functions) is

$$K_1(z) = \frac{1}{z} + \frac{z}{2} \left(\ln \frac{z}{2} + \gamma - \frac{1}{2} \right) + O(z^3 \ln z), \quad (\text{E87})$$

leading to, within terms of order $|a^2(\xi^2 + \kappa^2) \ln(a^2(\xi^2 + \kappa^2))|$,

$$F_2(\xi, a) = -i \left[\frac{1}{2} + \ln \frac{2}{a} - \gamma + \frac{1}{2} \frac{(\kappa_2^2 + \xi^2) \ln(\kappa_2^2 + \xi^2) - (\kappa_1^2 + \xi^2) \ln(\kappa_1^2 + \xi^2)}{\kappa_1^2 - \kappa_2^2} \right]. \quad (\text{E88})$$

Eq. (3.3) is evaluated using Eqs. (E88) and (E84) in the MATLAB program `findk0A.m`.

APPENDIX F: MATLAB PROGRAMS

Taking inputs of ϵ and a/h , the program `res5.m` calculates the first five resonant values of $\kappa_2 h$. For this it calls `resB.m` which in turn calls `nxtB.m`. The program `resB.m` supplies the error as part of its output, calculated using `ISD.m`. The computing of the integral over the kernel is done by the program `ISD.m` and the similar subroutine `ISDC` of `nxtB.m`. These call `K.m` which in turn calls `K1.m`, `K2.m`, `K3.m`. The program `K2.m` calls `K20.m` to get $\mathbf{K}_2(0)$, and `K3.m` calls `K31.m` and `Gj.m`. Many of these programs call `findk0A.m` to obtain $-i$ times the zero in the ξ -plane of the Fourier transform of the kernel $\mathbf{K}(x)$; that Fourier transform is accurately approximated by the subroutine `Ktilde` inside `findk0A.m`.

```
function[k0]=findk0A(ep,ell2,al,a_by_h)
%k here stands for \kappa
%al = - arg(k) al=pi/2 for propagation constant real
%(case of most interest)
% refines function[y]=findk0k2(a,krel)
```

```

% a is  $|k_2|a$  ; krel =  $k_1/k_2$ .
%gets zero from linear approx to a complex function.
%wj = w(zj)
zstart = i*exp(-i*al)*sqrt((1+ep)/2)*ell2*(1+.04i); %rough starting
%approx to  $X=\xi^2/|k_2|^2$  for square of zero
del = .1;
zst = zstart;

for ll= 1:7 %set to 1:7

z1 = zst+del;
w1 = Ktilde(ep,ell2,al,z1,a_by_h);
z2 = zst-del;
w2 = Ktilde(ep,ell2,al,z2,a_by_h);
yk1 = (w2*z1-w1*z2)/(w2-w1);
zst = yk1;
del = del/8;
end %for
test1 = Ktilde(ep,ell2,al,yk1,a_by_h);%shows error of found k_0
k0=-i*yk1;
k0tst=exp(i*al)*k0;
if imag(k0tst)<0
k0=-k0;
end
function[y]=Ktilde(ep,ell2,al,xi,a_by_h)
%29 July 2009: fix Ktilde3 of 7 June 2008 for arb  $|k_2|$ 
% k here stands for  $\kappa$ 
%al =  $\pi/2$  for real propagation constant (case of interest)

```

```

%WORKS FOR al near pi/2; not likely good otherwise!!!
%xi=\xi
%al = -arg(\kappa_2)
%Ktilde used for xi \approx \xi_0 \approx ...
% i*exp(-i*al)*ell2*sqrt(.5*(ep+1))*exp(i*delta), ...
% delta small and positive.
X=xi2;
ph=exp(i*al);
k2=ell2/ph;
k1=sqrt(ep)*k2;
k1sq=k12;
k2sq=k22;
ft1=k12+X;
ft2=k22+X;
log2=log(X+k2sq);%TEMPORARY FOR al near pi/2
log1=log(-X-k12)-i*pi;
gam = 0.5772156649015328; % from Abramowitz

%function[y]=F1(ep,ell2,al,xi,a_by_h)
fac1=1./(k1sq+k2sq);
T0= 2*(log(2/a_by_h)-gam);
k4=k2*sqrt(ep/(ep+1));
T1=(k2sq.*log1-k1sq.*log2)./(k1sq-k2sq);
rt3=sqrt(X+k42);
fac2=i*k1*k2*k4/((k1sq-k2sq)*rt3);
lograt2=log((rt3-i*k2*k4/k1)/(rt3+i*k2*k4/k1));
lograt1=log((i*k1*k4/k2-rt3)/(rt3+i*k1*k4/k2))-i*pi;
T2=fac2.*(lograt2-lograt1);

```

```

F1=fac1.*(T0+T1+T2);
%end

%function[fval]=F2(ep,ell2,al,xi,a_by_h)
f1 = -gam+log(2/a_by_h)+.5;
F2= f1+.5*(ft2*log2-ft1.*log1)./(k1sq-k2sq);
%end
y=X.*F1+F2;
end

end

```

```

function [yg]=Gj(j,ep,ell2,al,a_by_h,x)
%15 July 2009
%ell_j=abs(kappa_j)
%here k is for kappa; al = -arg(k2)=-arg(k1)
%ep is dielectric constant, ASSUMED REAL
k0=findk0A(ep,ell2,al,a_by_h);
k2=ell2*exp(-i*al);
k1=sqrt(ep)*k2;
if j==1
    R=k1/k2;
else R=k2/k1;
end
ell4=ell2*sqrt(ep/(ep+1));

```

```

k4=k2*sqrt(ep/(ep+1));
er=10-8;
rtf=sqrt(k02-k42); %from study of branch in 12 July note
bf =k4*R;
G2res = i*pi*k0*exp(-k0*x)*log((rtf-bf)/(rtf+bf))/rtf;
ulim = sqrt(1+R2)-1;
Int_term = -2*pi*i*quad(@itg2,0,ulim,er);
yg = G2res+Int_term;
    function y2= itg2(t)
        efac = exp(-exp(-i*al)*(t+1)*ell4*x);
        rrtf=1./sqrt(t.*(t+2));
        t1s=(t+1).^2;
        y2=t1s.*efac.*rrtf./(t1s-exp(2*i*al)*k02/ell42);
    end
end

```

```

-----

function yf=ISD(ep,ell2,al,a_by_h,n)
%compute
%\int_0^2 dx K(x)*2*(((n*pi/2)^2-k02)*(2-x)cos(.5*n*pi*x)
%-(4/(n*pi))*((n*pi/2)^2-k02)*sin(n*pi*x/2))
%27 July 2009
k0=findk0A(ep,ell2,al,a_by_h);
function yi=itg(t)
    f1=2*((.5*n*pi)^2+k02)*(2-t).*cos(.5*n*pi*t);

```



```

        f2=(4/(n*pi))*((.5*pi*n)^2-k02)*sin(.5*n*pi*t);
yi=K(ep,ell2,al,a_by_h,t).*(f1-f2);
end
er = 10^-9;
yf=quadv(@itg,0,2,er);
end

```

```

-----

function [y]=K(ep,ell2,alpha,a_by_h,xvec)
T1=K1(ep,ell2,alpha,a_by_h,xvec);
T2=K2(ep,ell2,alpha,a_by_h,xvec);
T3=K3(ep,ell2,alpha,a_by_h,xvec);
y=T1+T2+T3;
end

```

```

-----

function[y]=K1(ep,ell2,al,a_by_h,x)
%k for kappa; 21 July 2009
S=size(x);
rh=sqrt(a_by_h^2+x.^2);
%nsmall = 0;
k2=ell2*exp(-i*al);
k1=sqrt(ep)*k2;

%assume x a vector with monotonically increasing elements
nv =S(2); %number of elements in x

```

```

if rh(1)< .001
    nsmall=min(ceil(nv*.001/(10-8+rh(nv))),nv);
    nbig =nv-nsmall;
    if nsmall ==nv,
        y=K1small(rh);
    end
    rhsmall = rh(1:nsmall);
    rhbig=rh(nsmall+1:nv); %gets here only if nsmall<nv
    ysmall=K1small(rhsmall);
    ybig=K1big(rhbig);
    y=[ysmall ybig];
else
    y=K1big(rh);
end

function yf=K1small(rrh)
    fac =2./rrh-(4/3)*(k12+k1*k2+k22)/(k1+k2)+(k12+k22)*rrh/2;
    yf=pi*fac/(k12+k22);
end
function yff=K1big(rrh)
    t1=(1+k2*rrh).*exp(-k2*rrh);
    t2=(1+k1*rrh).*exp(-k1*rrh);
    yff= 4*pi*(t1-t2)./((k14-k24)*rrh.^3);
end
end

```

```

function [val]=K2(ep,ell2,al,a_by_h,x)
%accepts vector x
k0=findk0A(ep,ell2,al,a_by_h);
k2=ell2*exp(-i*al);
k1=sqrt(ep)*k2;
K2null=K20(ep,ell2,al,a_by_h);
S =size(x);
nx=S(2);
er=10-8;
T1=x;
delta=10-7;
    for jj=1:nx
        xtemp=x(jj);
        if xtemp>delta
            T1(jj)=quad(@itg,delta,xtemp,er)+corfun(delta,xtemp);
        else
            T1(jj)=corfun(xtemp,xtemp);
        end
    end
T2=K2null*cosh(k0*x);
%get correction for starting integration from delta
    function [cor]=corfun(del,xc)
f1= 2*pi/(k12+k22);
rat=del/a_by_h;
tcor11=log(rat+sqrt(rat2+1));
tcor12=-(2/3)*del*(k12+k22+k1*k2)/(k1+k2);
tcor1=tcor11+tcor12;
tcor2=a_by_h-sqrt(del2+a_by_h2);

```

```

cor=f1*(tcor1*sinh(k0*xc)+tcor2*cosh(k0*xc));
    end %corfun
val=(k0-.5*(k12+k22)/k0)*T1+T2;
function yi=itg(t)
yi=sinh(k0*(xtemp-t)).*K1(ep,ell2,al,a_by_h,t);
end
end

```

```

-----

function yK=K3(ep,ell2,alpha,a_by_h,xvec)
%ell_j=abs(kappa_j)
%accepts xvec as a vector of values of x
%here k is for kappa; al = -arg(k2)=-arg(k1)
%ep is dielectric constant, ASSUMED REAL
k0=kappa0h(ep,ell2,alpha,a_by_h);
k2=ell2*exp(-i*alpha);
k1=sqrt(ep)*k2;
ell4=ell2*sqrt(ep/(ep+1));
k4=k2*sqrt(ep/(ep+1));
S =size(xvec);
nx=S(2);
yK=xvec;
for jj=1:nx
    x=xvec(jj);
    K32=i*k1*k2*k4*(Gj(2)-Gj(1))/(k14-k24);
    KK31=K31(ep,ell2,alpha,a_by_h,x);
    yK(jj)=K32+KK31;

```

```

end
function [yg]=Gj(j)
%15 July 2009
if j==1
    R=k1/k2;
else R=k2/k1;
end
%lim =100*pi;
er=10-8;
rtf=sqrt(k02-k42); %from study of branch in 12 July note
bf =k4*R;
G2res = i*pi*k0*exp(-k0*x)*log((rtf-bf)/(rtf+bf))/rtf;
ulim = sqrt(1+R2)-1;
Int_term = -2*pi*i*quad(@itg2,0,ulim,er);
yg = G2res+Int_term;
    function y2= itg2(t)
        efac = exp(-exp(-i*alpha)*(t+1)*ell4*x);
        rrtf=1./sqrt(t.*(t+2));
        t1s=(t+1).^2;
        y2=t1s.*efac.*rrtf./(t1s-exp(2*i*alpha)*k02/ell42);
    end
end

end

-----

function[y] =K20(ep,ell2,al,a)

```

```

%PRIMARY
%k for kappa; a for a/h
%to evaluate  $K_-(x,a)|_{x=0}$  10 June 2009
%find k0 using  $\kappa_0 = -ik_0(i\kappa_1, i\kappa_2)$ 
%which follows from rule that  $\kappa_j = -i k_j$ 
k2=ell2*exp(-i*al);
k1 =sqrt(ep)*k2;
k0=findk0A(ep,ell2,al,a);
C=pi*(1-2*k02/(k12+k22))/(k12-k22);
%T1=2*(exp(-k1*a)-exp(-k2*a))/a;
%T2=2*(kf(k2)-kf(k1))/(k0*a);
%T3= k1-k2+lnf(k2)-lnf(k1);
%K20def=C*(T1+T2+T3)
gam = 0.5772156649015328;
T1S=k2-k1-(k12-k22)*(log(a/2)+gam-.5)/k0;
T2S=((k22-k02)*log(k2+k0)-(k12-k02)*log(k1+k0))/k0;
y=C*(T1S+T2S);
end

-----

function [yK31]=K31(ep,ell2,al,a_by_h,x)
%check; 17July09
%k for kappa
k2=exp(-i*al)*ell2;
k1=sqrt(ep)*k2;
%ell1=sqrt(ep)*ell2;
%%%

```

```

k0=findk0A(ep,ell2,a1,a_by_h);
%er=10-9;
%T311=2*pi*(exp(-k2*x)-exp(-k1*x))./x;

%calculate T312
%if for CASE OF x SMALL
%a=exp(i*a1);
t2=pi*(log((k12-k02)/(k02-k22))+i*pi)*exp(-k0*x)/k0;
if x<.0001
    e1=-log(k1-k0);
    e2=-log(k2-k0);
    if imag(k2-k0)>0
        e2=e2+2*pi*i;
    end
    e1p=-log(k1+k0);
    e2p=-log(k2+k0);
else
    e1=expint((k1-k0)*x);
    e2=expint((k2-k0)*x);
    if imag(k2-k0)>0
        e2=e2+2*pi*i;
    end
    e1p=expint((k1+k0)*x);
    e2p=expint((k2+k0)*x);
end

e0x=exp(k0*x);
t5form=pi*((e1-e2)./e0x-(e1p-e2p).*e0x)/k0; %as in branch/ckT312

```

```

T312=t2+t5form;
% end T312 (from Eq.(1.18) of 20July res5.tex
fn2=-k0*(k12+k22-k02)*(k0*T312/pi);
if x < .001
    tt1=(2*(k12+k22)-k1*k2)/3-k02;
    tt2=k02-.5*(k12+k22);
    f1=2*(k1-k2)*tt1+x*(k12-k22)*tt2;
    yK31=pi*(f1+fn2)/(k14-k24)+pi*k0*exp(-k0*x)/(k12+k22);
else
    f1=(k02-k22+2*k1./x+2./x.^2).*exp(-k1*x);
    f2=(k02-k12+2*k2./x+2./x.^2).*exp(-k2*x);
    fn1=2*(f1-f2)./x;
    yK31=pi*(fn1+fn2)/(k14-k24)+pi*k0*exp(-k0*x)/(k12+k22);
%CHECK K31 for values of alpha < pi/2
%K31def=2*quad(@itg,0,pi*70/x,er)/(k14-k24)
%function[yi]=itg(t)
%fac1=cos(t*x)./(t.^2+k02);
%fac2=(k12+k22+t.^2).*log((k12+t.^2)./(k22+t.^2))-k12+k22;
%yi=fac1.*fac2;
end
end

```

```

-----

function y=kappa0h(ep,ell2,alpha,a_by_h)
%ASSUME 0 <= alpha < pi Modified 18 July 2009
%ell2 = abs(kappa_2)*h
y=-i*kh0(ep,exp(i*(.5*pi-alpha))*ell2,a_by_h);

```



```

yt=exp(i*alpha)*y;
if imag(yt)<0
    y=-y;
end

function khVal = kh0(ep,k2h,aBYh)%15 July 2009
%find khVal = k_2h where k_2 is the zero in zeta-plane of
%Fourier x-form of kernel, as approximated by
%Tai's formula (4.28,11) of May 2008, p24
%khValSq = khVal2;
% reference case is ep=4.
rt4=sqrt(.5*(ep+1));
E=.5*pi*(.5*(ep+1)-ep/rt4)/(ep-1) ...
    -i*(.5-(ep/((ep-1)*rt4))*log((ep+rt4)/(1+rt4)));
gamVal = -psi(1); %Euler's constant 0.5772156 ...
den= log(aBYh*sqrt((ep-1)*k2h.^2/2))+gamVal -log(2)-i*pi*.5;
khValSq= k2h.^2*.5*(ep+1).*(1-i*E./den);
khVal=sqrt_dn(khValSq);

function y=sqrt_dn(x)
y=exp(i*pi/4)*sqrt(-i*x);
end

end

%tested against k2h=exp(i*phi) for phi=linspace(-.4,1.6)
%no jumps found, so branch cuts seem not to cause trouble.
% 13 June 2009
end

```

```

-----

function kappa2_nxt=nxtB(ep,ell2S1,alS,inc,a_by_h,n)
%S for "start"
ell2S2=ell2S1+inc;
kappa2S1=ell2S1*exp(-i*alS);
kappa2S2=ell2S2*exp(-i*alS);
fn1=ISDC(ep,ell2S1,alS,a_by_h,n);
fn2=ISDC(ep,ell2S2,alS,a_by_h,n);
kappa2_nxt=findX(kappa2S1,kappa2S2,fn1,fn2);
function z=findX(z1,z2,fn1,fn2)
z=z1-fn1*(z2-z1)/(fn2-fn1);
end

function yf=ISDC(ep,ell2,al,a_by_h,n)
%compute
%\int_0^2 dx K(x)*2*(((n*pi/2)^2-k0^2)*(2-x)*cos(.5*n*pi*x)
%-(4/(n*pi))*((n*pi/2)^2-k0^2)*sin(n*pi*x/2))
%27 July 2009
k0=findk0A(ep,ell2,al,a_by_h);
%k0=kappa0h(ep,ell2,al,a_by_h); Crude by reliable for test
function yi=itg(t)
    f1=2*(((.5*n*pi)^2+k0^2)*(2-t).*cos(.5*n*pi*t);
    f2=(4/(n*pi))*((.5*pi*n)^2-k0^2)*sin(.5*n*pi*t);
yi=K(ep,ell2,al,a_by_h,t).*(f1-f2);
end
er = 10^-8;
yf=quadv(@itg,0,2,er);

```

end

end

```
num = 300;
x=linspace(0,20,num);
KV04=x;
KV06=x;
for jj=1:num
KV04(jj)=K(4,1,pi/2,10-4,x(jj));
KV06(jj)=K(4,1,pi/2,10-6,x(jj));
end
Y04=imag(KV04);
Y06=imag(KV06);
plot(x,Y04,x,Y06,'--')
axis([0 20 -.5 .5])
xlabel('k_2x')
ylabel('Components of kernel K(k_2x)')
title('Comparison of kernel for a/h=10-4 vs. 10-6')
```

```
function [k2hres]=res5(ep,a_by_h)
k2hres=ones(1,5); %k is for k not for kappa
err_n=k2hres;
for n=1:5
    val=resB(ep,a_by_h,n);
```

```

        k2hres(n)=val(1);
        err_n(n)=val(2);
end
errVec = err_n
end

-----

function[k2reswE]=resB(ep,a_by_h,n)
%28 July 2009 n=n_res
%NEED more checking if dielectric constant ep complex!
alS = pi/2+.04;
ell2S1=.5*n*pi/sqrt((ep+1)/2);
inc=.02;

for jj=1:4
kappa2_nxt=nxtB(ep,ell2S1,alS,inc,a_by_h,n);
ell2_nxt = abs(kappa2_nxt);
al_nxt = argM(kappa2_nxt);
ell2S1=ell2_nxt;
alS=al_nxt;
inc=inc/7;
end
kappa2res=kappa2_nxt;
k2res = i*kappa2res;
%err=0 % speed up in exchange for loss of error info
err=ISD(ep,ell2_nxt,al_nxt,a_by_h,n);
k2reswE=[k2res err];

```

```

function ya = argM(z)%gets al s.t.  $z = |z| \cdot \exp(-i \cdot al)$ 
%with  $0 \leq al < 2 \cdot \pi$ 
r=abs(z);
y=imag(z);
x=real(z);
if y <=0
    if x >0
        ya = -asin(y/r);
    else
        ya=pi+asin(y/r);
    end
else
    if x >0
        ya=2*pi-asin(y/r);
    else
        ya = pi+asin(y/r);
    end
end
end %argM
end

```

REFERENCES

- [1] R. W. P. King, *The Theory of Linear Antennas* (Harvard University Press, Cambridge, MA, 1956).
- [2] R. W. P. King, M. Owens, and Tai Tsun Wu, *Lateral Electromagnetic Waves* (Springer-Verlag, New York, 1992).
- [3] R. W. P. King and C. W. Harrison, Jr., *Antennas and Waves* (M. I. T. Press, Cambridge, MA, 1968), pp. 445–447.
- [4] E. Erdélyi, ed., *Higher Transcendental Functions*, vol. II (McGraw-Hill, New York, 1953).
- [5] E. Erdélyi, ed., *Higher Transcendental Functions*, vol. I (McGraw-Hill, New York, 1953).

REPORT DOCUMENTATION PAGE			Form Approved OMB NO. 0704-0188	
Public Reporting burden for this collection of information is estimated to average 1 hour per response, including the time for reviewing instructions, searching existing data sources, gathering and maintaining the data needed, and completing and reviewing the collection of information. Send comment regarding this burden estimates or any other aspect of this collection of information, including suggestions for reducing this burden, to Washington Headquarters Services, Directorate for information Operations and Reports, 1215 Jefferson Davis Highway, Suite 1204, Arlington, VA 22202-4302, and to the Office of Management and Budget, Paperwork Reduction Project (0704-0188,) Washington, DC 20503.				
1. AGENCY USE ONLY (Leave Blank)		2. REPORT DATE November 12, 2009		3. REPORT TYPE AND DATES COVERED Technical Report 1 Aug 2008–31 Jul 2009
4. TITLE AND SUBTITLE Electromagnetic Resonances of a Wire on an Earth-Air Interface			5. FUNDING NUMBERS Grant W911NF-07-1-0509 Project 5276140-01	
6. AUTHOR(S) John M. Myers, Sheldon S. Sandler, and Tai Tsun Wu (PI)				
7. PERFORMING ORGANIZATION NAME(S) AND ADDRESS(ES) President & Fellows of Harvard College School of Engineering and Applied Sciences, Cambridge, MA 02138			8. PERFORMING ORGANIZATION REPORT NUMBER	
9. SPONSORING / MONITORING AGENCY NAME(S) AND ADDRESS(ES) U. S. Army Research Office P.O. Box 12211 Research Triangle Park, NC 27709-2211			10. SPONSORING / MONITORING AGENCY REPORT NUMBER	
11. SUPPLEMENTARY NOTES The views, opinions and/or findings contained in this report are those of the author(s) and should not be construed as an official Department of the Army position, policy or decision, unless so designated by other documentation.				
12 a. DISTRIBUTION / AVAILABILITY STATEMENT Approved for public release; distribution unlimited.			12 b. DISTRIBUTION CODE	
13. ABSTRACT (Maximum 200 words) A promising approach to detecting roadside bombs attached to command wires is the electromagnetic sensing and identification of the wires. The lowest five resonant frequencies of the wires, along with the widths of the resonances, can serve as a "fingerprint" for finding the wires. A first large step toward exploiting this fingerprint is to calculate the resonances and their widths for a straight wire on a flat interface between a homogeneous earth and air. The calculation of resonances requires extending the theory of the linear antenna to deal with a wire on the interface between two dielectric media, which we accomplish here. Complex-valued resonant frequencies are defined as those for which a certain homogeneous integral equation for the current in the strip on the interface has non-trivial solutions. By applying a Galerkin procedure we obtain approximate numerical solutions for the resonant frequencies and their widths. A table of resonances is given for the case of a relative dielectric constant of the earth equal to 4 and for three values of the ratio of wire radius to wire length. MATLAB computer programs for determining resonant frequencies and widths for other parameter values are included.				
14. SUBJECT TERMS Command wires on the earth; theory of linear antenna on planar interface; integral equations of Pocklington and Hallen type; resonant frequencies; numerical calculations; Galerkin method; MATLAB computer programs.			15. NUMBER OF PAGES 69	
			16. PRICE CODE	
17. SECURITY CLASSIFICATION OR REPORT UNCLASSIFIED	18. SECURITY CLASSIFICATION ON THIS PAGE UNCLASSIFIED	19. SECURITY CLASSIFICATION OF ABSTRACT UNCLASSIFIED	20. LIMITATION OF ABSTRACT UL	

NSN 7540-01-280-5500

Standard Form 298 (Rev.2-89)
Prescribed by ANSI Std. Z39-18
298-102

Enclosure 1